Nucleospin Extract II (Macherey-Nagel GmbH and Co. KG, Düren, Germany) according to the manufacturer's recommendations. The conversion reaction was completed by desulfonating in 0.3 N NaOH for 20 min at 37°C. The DNA was ethanol precipitated, then washed by 70% ethanol and resuspended in TE buffer. Primers for bisulfite genomic sequencing PCR were designed by the use of the online program MethPrimer. The primers for region 1 were: 5'-TTT GAAGGGTTTTGGGTTTAATATAT-3' (forward) and 5'-CTCCTAACTACAAACTATCCAACAC-3' (reverse). The primers for region 2 were: 5'-GGGTTGGTTTTAAGTTT AGGGATAG-3' (forward) and 5'-AAAAAAAATTCTA TAACTCATCCAC-3' (reverse). The primers for region 3 were: 5'-TGTATATTGATGGAGGAGGTATAGT-3' (forward) and 5'-AAAAAAAACTAAAAATCTTCTCCC-3' (reverse). The primers for region 4 were: 5'-TGGAGAAGG TTTTGAGTATGTTTTT-3' (forward) and 5'-CCACAT CTATCCCTATAACCACATC-3' (reverse). The amplification products were checked by electrophoresis. After gel purification, the PCR products were cloned into pCR2.1-TOPO vector (Invitrogen), and 10 or more colonies were randomly chosen and sequenced. Methylation level analysis was performed by using QUMA software (http://quma.cdb.riken.jp/).

Construction of HSPB7 expression vector. To construct an HSPB7 expression vector, the entire coding sequence of HSPB7 cDNA (based on NM_014424.4 in Pubmed) was amplified by PCR using KOD-Plus DNA polymerase (Toyobo, Osaka, Japan). The primers used for PCR reaction were 5'-AAAGAATTCCGTCCGTGGATGAGCCACAG-3' (forward) and 5'-TTTCTCGAGGATTTTGATCTCCGTC CGGA-3' (reverse). The PCR product was inserted into the *Eco*RI (Takara) and *Xho*I (Takara) sites of pCAGGSnHC expression vector containing the HA tag. The sequence and protein expression for pCAGGSnHC-HSPB7-HA were confirmed by DNA sequencing, western blot and ICC analyses.

Western blot analysis. To prepare whole cell extracts, cells were collected and lysed in chilled radioimmunoprecipitation assay buffer (RIPA) (50 mM Tris-HCl at pH 8.0, 150 mM sodium chloride, 0.1% SDS, 0.5% DOC, 1% NP-40), 1 mM phenyl methylsulphonyl fluoride (PMSF), 1 mM DTT and 0.1% Calbiochem Protease Inhibitor Cocktail Set III, EDTA-Free (EMD Chemicals Inc., Merck KGaA, Darmstadt, Germany). Following 15-min ultrasonication and subsequent 30-min incubation on ice, homogenates were centrifuged for 15 min at 4°C, and the supernatants were collected and boiled in SDS sample buffer. Each sample was loaded into a 15% SDS-polyacrylamide gel electrophoresis (SDS-PAGE) and transferred to a nitrocellulose membrane (Hybond™ ECL™, Amersham, Piscataway, NJ, USA). Protein bands on western blots were visualized by chemiluminescent detection (ECL, Amersham). The primary antibodies used in this study included rabbit anti-human HSPB7 polyclonal antibody (Proteintech, diluted 1:500) and goat anti-rabbit IgG-HRP secondary antibody (Santa Cruz Biotechnology, Santa Cruz, CA, USA, diluted 1:30,000).

Immunocytochemistry (ICC). Five RCC cell lines were seeded on Lab-Tek II chamber slide system (Nalge Nunc International). At day 5 after the 5-Aza-2'-dC-treatment, the cells were fixed with 4% paraformaldehyde in PBS for 10 min and permeabilized with 0.2% Triton X-100 in PBS for 5 min at room temperature. Cells were covered with blocking solution (3% BSA in PBS contained 0.2% Triton X-100) for 60 min at room temperature. Then the cells were incubated with rabbit anti-human HSPB7 polyclonal antibody (Proteintech, diluted 1:250) overnight at 4°C, following an Alexa Fluor 488 goat anti-rabbit IgG antibody (Molecular Probes, Eugene, OR, USA, diluted 1:1,000) for 1 h at room temperature. PBS or 0.2% Triton X-100 in PBS was used for washing after each step. Then cells were stained with DAPI (Vector) and viewed with a laser scanning spectral confocal microscope (Leica TCS SP2).

Colony formation assay. Cells were plated in a 6-well plate and transfected with pCAGGSnHC-HSPB7-HA or empty vector using FuGENE 6 (ACHN and Caki-1) or lipofectamine LTX (Caki-2, A498 and 786-O) transfection reagent (Roche). After 48 h of transfection, cells were selected with G418 (Gibco) for 14-21 days. Colonies (>1 mm diameter) were counted using the Image J software after fixed with methanol and stained with 0.1% crystal violet. The experiment was carried out twice in duplicate wells.

DNA-damaging treatments. When cells reached 60-70% confluence in the culture dish, HCT116 ($p53^{-/-}$) and HCT116 ($p53^{+/+}$) cells were incubated with adriamycin for 2 h at the indicated concentration. The cells were harvested at different time points after cell-damaging treatment as indicated in the figure legends. Replication-deficient recombinant adenovirus encoding p53 (Ad-p53) or LacZ (Ad-LacZ) was generated and purified as previously described (18,19). NCI-H1299 lung cancer cells were infected with viral solutions at an indicated multiplicity of infection (MOI) and incubated at 37°C until harvest.

p53-binding site screening by Luciferase assay. Two DNA fragments including candidate p53-binding sites of HSPB7 were amplified by PCR, digested with *Mlu*I and *Bgl*II and cloned into pGL3-Promoter vector (Promega, Madison, WI, USA). Primer sequences (including *Mlu*I and *Bgl*II site) for p53-binding sites of HSPB7 were: region 1 forward, 5'-AAAACGCGTTCCAAGGTCACACAGCAGAG-3'; and reverse, 5'-TTTAGATCTGCTTCAAACCGGTCATCCT-3'; and region 2 forward, 5'-AAAACGCGTTGAGCAGGAGCA GTCAGAGA-3'; and reverse, 5'-TTTAGATCTAGCCCCAAG AGGACAAAGTT-3'.

H1299 cells were seeded in 12-well plates ($5x10^4$ cells per well). Twenty-four hours later, cells were co-transfected with i) 25 ng of the pRL-CMV vector (Promega) (for internal control); ii) 125 ng of either pcDNA3.1(+)-wild-type p53 or pcDNA3.1(+) empty vector; and iii) 125 ng of pGL3-promoter vector with either the p21 promoter region corresponding to p53-binding site (for positive control) (20), that with p53-binding site 1 of HSPB7, that with p53-binding site 2 of HSPB7, or pGL3-Promoter mock vector (for negative control) by using FuGENE 6 transfection reagent (Roche). After 36-h incubation, luciferase activity was measured using the Dual Luciferase Assay System (Promega) (21).

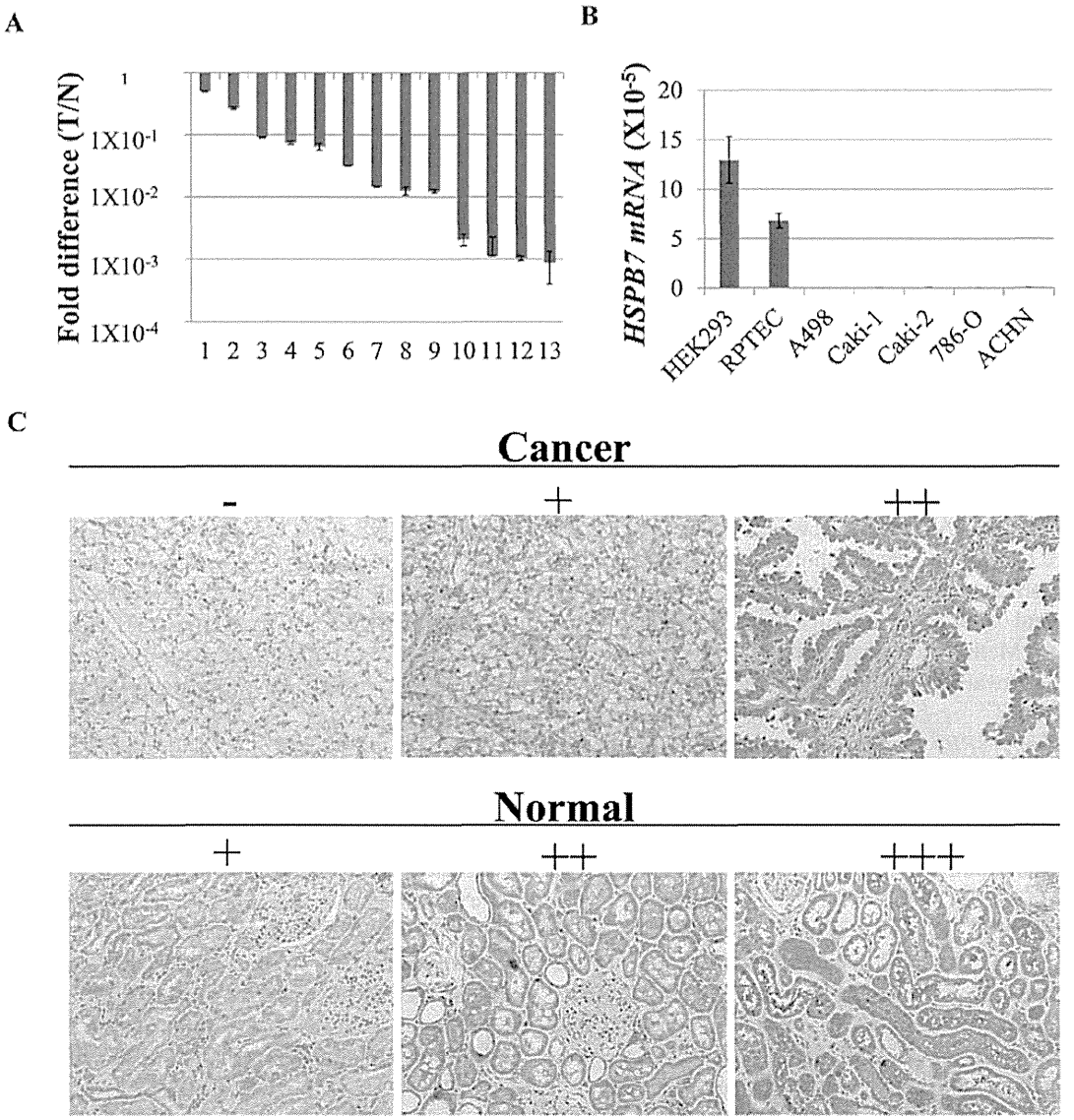

Figure 1. Downregulation of HSPB7 in RCC. qPCR analysis shows that HSPB7 mRNA expression was significantly downregulated (A) in 11 (85%) of 13 RCC tissues compared with the normal renal tissue, and (B) in all the five RCC cell lines compared with normal HEK 293 and RPTEC cells. T and N represent RCC tissue sample and normal renal tissue, respectively. B2M (β2 microglobulin) was used for normalization of expression levels. Values are expressed as the mean ± SD. (C) IHC analysis of a tissue array consisting of 11 pairs of human RCC sample reveals that the expression of HSPB7 was significantly higher in normal kidney tissues than in RCC tissues. According to the intensity of HSPB7 staining, these samples were evaluated as: negative (-), weakly positive (+), moderate positive (++), and strong positive (+++). HSPB7 negative or weakly positive (-/+) were considered low expression, and moderate or strong positive were considered high expression (++/+++). Summary of the IHC results is shown in Table I.

Statistical analysis. All statistical analyses including t-test and Fisher's exact test were carried out by using the SPSS software (version 17). Data are shown as mean ± SD. All tests were 2-sided and p-value of <0.05 was considered to indicate a statistically significant difference.

Results

Downregulation of HSPB7 in RCC. Based on the analysis of microarray data of 15 clear cell renal cell carcinomas, we found HSPB7 to be significantly and commonly downregulated in RCC. qPCR experiment confirmed its downregulation in 11 (85%) of 13 RCC tissues and in all of the five RCC cell lines (Fig. 1A and B), compared with their corresponding normal controls. IHC analysis of a tissue array consisting of 11 pairs of human RCC sample revealed that the expression of HSPB7 was significantly higher in normal kidney tissues than that in RCC tissues (Fig. 1C and Table I). We also detected HSPB7 expression mainly in the cytoplasm of normal renal tubular epithelial cells. To explore the expression patterns of HSPB7 in other normal tissues, we performed qPCR analysis using mRNAs isolated from 25 normal tissues. HSPB7 expression was detected ubiquitously in human tissues (Fig. 2).

5-Aza-dC treatment restores HSPB7 expression in RCC cell lines. To investigate whether the methylation status of the HSPB7 gene could affect HSPB7 expression in RCCs, 5 RCC cell lines, Caki-1, Caki-2, ACHN, 786-O and A498 were

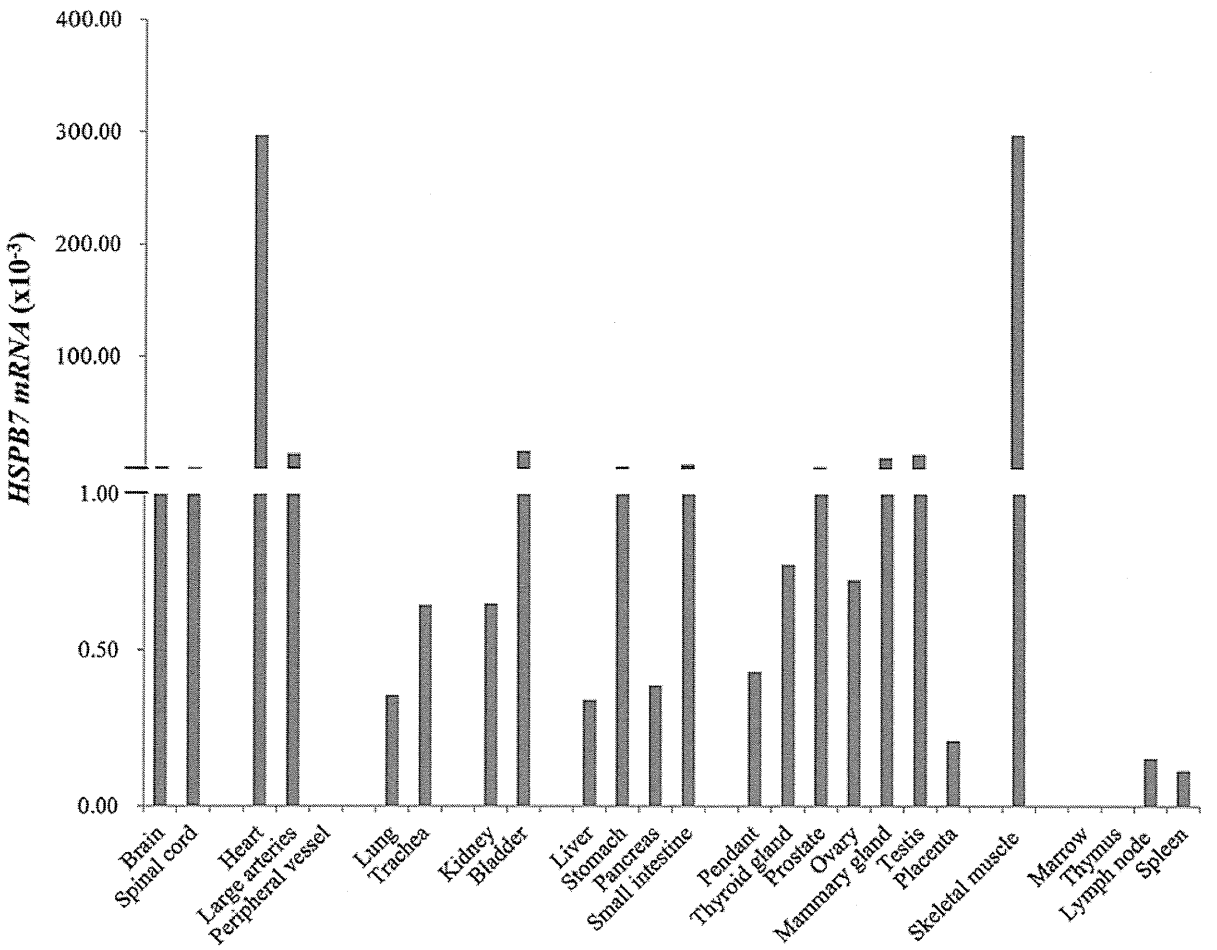

Figure 2. HSPB7 expression levels in normal tissues. qPCR analysis of HSPB7 was performed using mRNA isolated from 25 different normal tissues. B2M was used for normalization of expression levels.

treated with a demethylating agent 5-Aza-dC, and then the expression levels of HSPB7 were analyzed by qPCR, western blot and IHC analysis. We found that HSPB7 mRNA expression were restored in all the 5 RCC cell lines by the treatment with 5-Aza-dC (Fig. 3A), and the HSPB7 protein expression could also be detected in two cell lines, 786-O and A498, in which mRNA expression was most highly induced (Fig. 3B), indicating suppression of HSPB7 in RCC was caused probably by DNA hypermethylation. We performed exon sequencing of HSPB7 in these five RCC cell lines, but no mutation or deletion/insertion was detected (data not shown).

Hypermethylation of HSPB7 in RCC. To confirm the methylation status of the HSPB7 gene, bisulfite sequencing was performed for the 5 RCC cell lines Caki-1, Caki-2, ACHN, 786-O and A498 as well as 2 normal renal cell lines RPTEC and HEK293. We first screened two CpG islands, regions 1 and 2 shown in Fig. 3C, but no significant difference of methylation status was found in these two regions in normal and cancer cell lines. Then, we performed the second screening for regions 3 and 4 (Fig. 3C) (we also screened the other regions in normal cells, but data are not shown). In region 4, we found significantly higher levels of methylation in the 5 RCC cell lines than in the 2 normal renal cell lines.

Table I. Immunohistochemical expression of HSPB7 in RCC tissue array.

	Total	Low (-/+)	High (++/+++)	Fisher's t-test
Clear cell				
Cancer	9	7	2	P=0.015
Normal	9	1	8	
Papillary				
Cancer	2	1	1	-
Normal	2	0	2	
Total				
Cancer	11	8	3	P=0.008
Normal	11	1	10	

All tests were 2 sided and P<0.05 was considered to indicate a statistically significant difference.

Ectopic HSPB7 expression suppresses RCC cell clonogenicity. To study the effect of HSPB7 expression on tumor growth, Caki-1 and ACHN cells were transfected with HSPB7 expres-

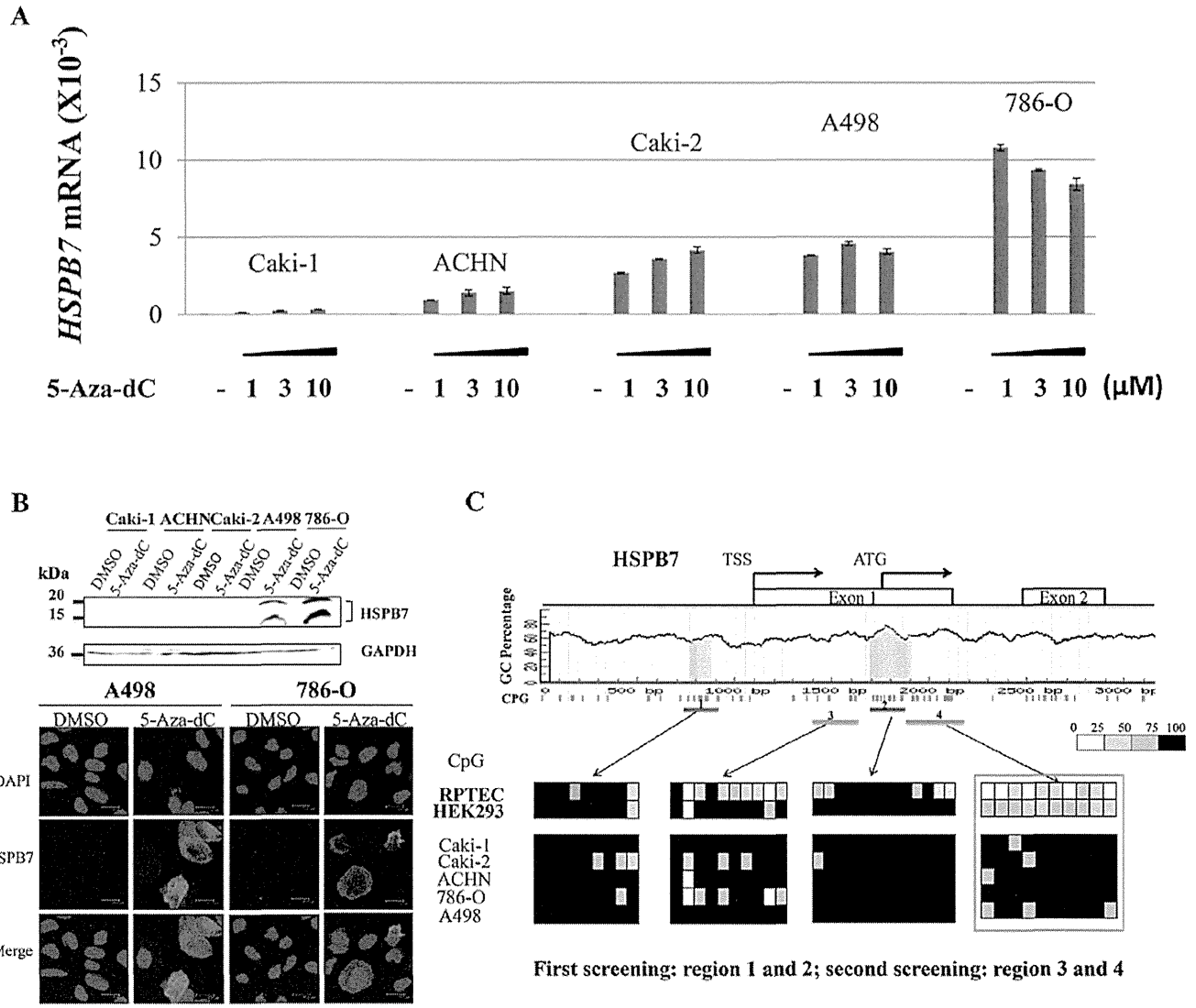

Figure 3. Epigenetic silencing of HSPB7 in RCC cell lines. (A) qPCR analysis and (B) western blot and ICC analysis of HSPB7 were performed in five RCC cell lines with treatment of the demethylating agent 5-Aza-dC. B2M was used for normalization of mRNA expression levels. GAPDH was used for normalization of protein expression levels. Values are expressed as the mean ± SD. (C) Hypermethylation of HSPB7 was confirmed by means of bisulfite sequencing. For each of the regions 1-4 in the cell lines, 10 or more colonies were randomly chosen and sequenced. Each square indicates a CpG site, and an average methylation level per CpG site is indicated by % methylation (shown in different color): white, 0-25% methylation; bright grey, 26-50% methylation; dark grey, 51-75% methylation; and black, 76-100% methylation. Region 4 showed higher level of methylation in the five RCC cell lines (Caki-1, Caki-2, ACHN, 786-O and A498) than in the two control cell lines (RPTEC and HEK293).

sion vector, pCAGGSnHC-HSPB7-HA. Introduction of HSPB7 into these two cancer cell lines caused significant decrease in the number of colonies, compared with corresponding mock-transfected controls (Fig. 4A). We also performed colony formation assay in 3 other RCC cell lines (Caki-2, A498 and 786-O) using the same vectors, and confirmed similar growth-suppressive effects (Fig. 4B), implying that HSPB7 may function as a tumor suppressor gene.

HSPB7 is regulated by p53. To further elucidate the biological significance, we first investigated its possible involvement in the p53-pathway because α B-crystallin, one of the small heat shock protein family members, was reported to be induced by p53 (22,23). We applied qPCR analysis to evaluate the expression of HSPB7 in NCI-H1299 (p53 null) cell lines with or without introduction of p53 using the adenovirus system. After the infection of Ad-p53, we observed induction of HSPB7 in a dose- and time-dependent manner (Fig. 5A and B), while no induction was observed in the control cells. After the 48-hour treatment with 40 MOI of Ad-p53, the expression level of HSPB7 became nearly 5 times higher than the control cells (Fig. 5A). Induction of HSPB7 was also confirmed under the treatment with relative lower dose of Ad-p53 (8 MOI) at different time points. Concordantly, DNA damage by adriamycin treatment induced HSPB7 expression in HCT116 cells with wild-type p53, but not in HCT116 cells without wild-type p53 (Fig. 5C and D), indicating that HSPB7 expression is regulated by wild-type p53. To further investigate whether HSPB7 is directly regulated by p53, we screened two possible p53-binding sites indicated by the p53-binding site search

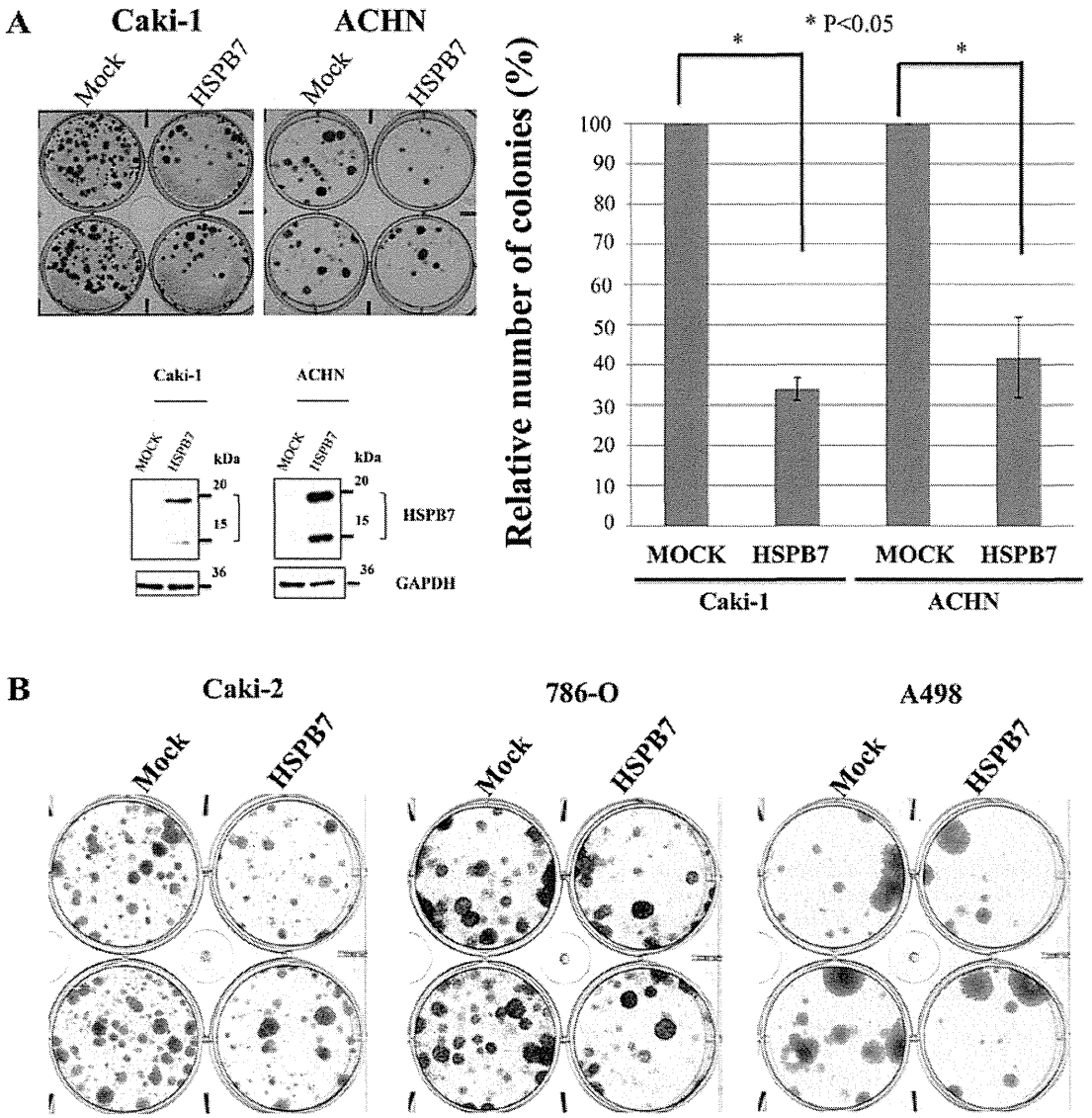

Figure 4. Ectopic HSPB7 expression suppresses RCC cell growth. (A) Colony formation assay showed that introduction of HSPB7 impaired colony-forming ability of Caki-1 and ACHN cells. Cells were transfected with plasmid expressing HSPB7 or mock plasmid, and colonies (>1 mm diameter) were counted after selection of 2-3 weeks with G418. At 48 h after transfection, total protein of cells was collected and applied for western blot to confirm the successful transfection. GAPDH was used for the normalization of protein expression levels. (B) Colony formation assay in Caki-2, 786-O and A498 RCC cell lines. Values are expressed as the mean ± SD.

software developed by us, but neither of these two candidate sites was confirmed to be a direct p53-binding site (data not shown). Although there might be another site(s) that p53 binds to, we are unable to conclude whether HSPB7 is directly or indirectly regulated by p53, it is certain that HSPB7 expression is inducible by wild-type p53.

Discussion

Scarce knownledge exists on the biological function of HSPB7, a member of the small heat shock protein family that is characterized by possessing a conserved α-crystallin domain. HSPB7 has been shown to interact with the cytoskeletal protein α-filamin (24) as well as other small heat shock proteins (25). HSPB7 belongs to a non-canonical HSPB protein that prevents the aggregation of polyQ proteins in an active autophagy machinery, but overexpression of HSPB7 alone did not affect the autophagy event (26). Several genome-wide association studies found that SNPs in the HSPB7 gene were strongly associated with idiopathic cardiomyopathies and heart failure (27-31). Recently, HSPB7 was suggested to regulate early developmental steps in cardiac morphogenesis (32). However, the involvement of HSPB7 in carcinogenesis has not been described.

Through the genome-wide expression analysis in RCCs, we identified HSPB7 as a candidate tumor suppressor gene because of its common and significant downregulation in RCCs. Subsequent functional analysis revealed that HSPB7 was downregulated in cancer cells by hypermethylation. Bisulfite sequencing of genomic regions of HSPB7 confirmed hypermethylation in RCC cell lines. Although region 4 (Fig. 3C) contained no CpG Island, we observed significantly

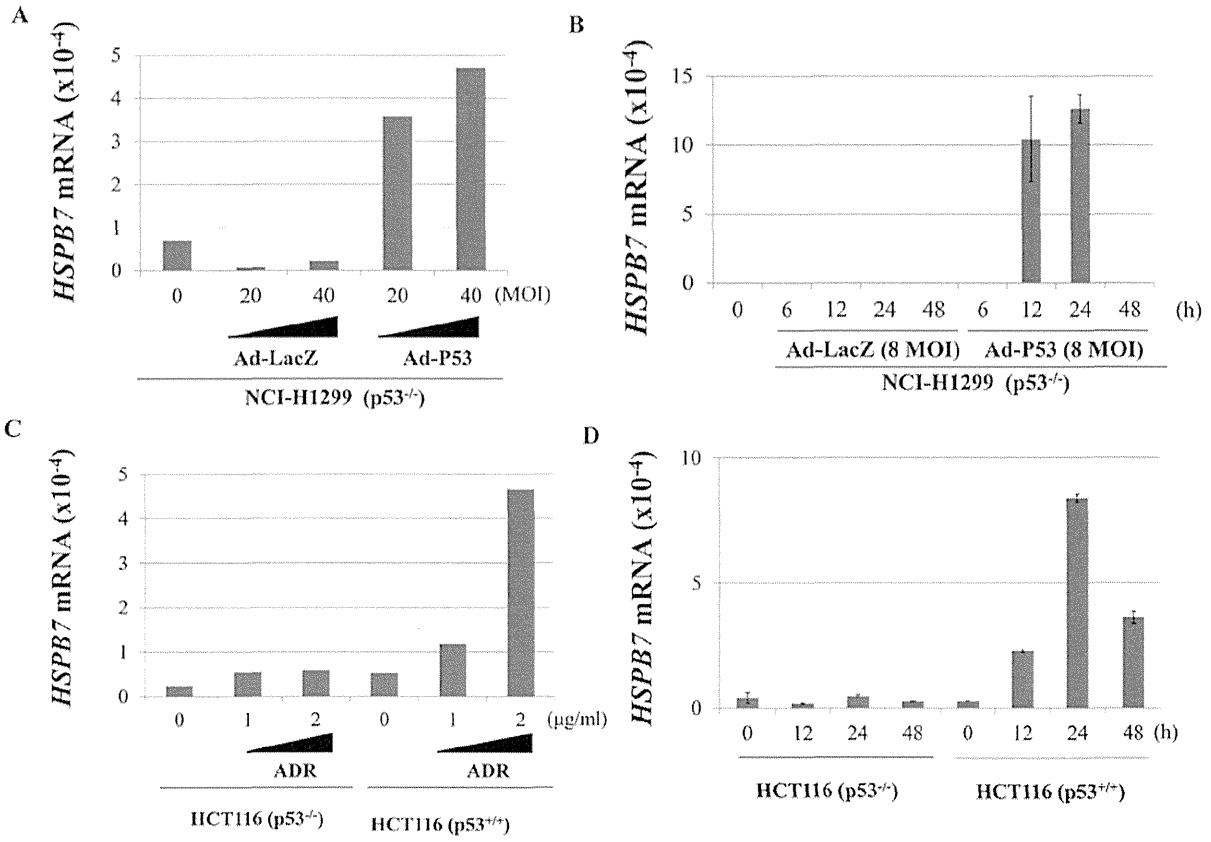

Figure 5. HSPB7 is regulated by p53. (A and B) HSPB7 expression in NCI-H1299 cells with or without p53 induction (A) dose- and (B) time-dependently. Cells were infected with replication-deficient recombinant adenovirus encoding p53 (Ad-p53) or LacZ (Ad-LacZ) at indicated doses, and the cells were collected 48 h later and qPCR analysis was performed (A). The cells were infected at 8 MOI and collected at different time points (B). (C and D) HSPB7 expression in HCT116 (p53$^{-/-}$) and HCT116 (p53$^{+/+}$) cells treated with adriamycin at indicated doses for 2 h and the cells were harvested at 48 h (C). The cells were treated with adriamycin at 2 μg/ml for 2 h and then harvested at different time points (D). B2M was used for normalization of expression levels. Values are expressed as the mean ± SD.

higher level of methylation in RCC cell lines than normal cell lines. Consistently, restoration of HSPB7 expression was observed by the treatment of cancer cells with 5-Aza-dC. In addition, since no somatic changes in coding regions of the HSPB7 gene were found in our sequence analysis of RCC cell lines or in the COSMIC database, HSPB7 in RCC is considered to be downregulated mostly by hypermethylation.

The second key finding in this study is that HSPB7 showed growth suppressive effect in cancer cells. Ectopic expression of HSPB7 significantly impaired colony-forming ability for 5 RCC cell lines, indicating that HSPB7 may function as a tumor suppressor gene. Similarly α B-crystallin, one of the small heat shock protein family members, was also indicated to function as a tumor suppressor in nasopharyngeal carcinoma cells (33). Furthermore, the region on chromosome 1p36.23-p34.3, where HSPB7 is located, showed frequent loss of heterozygosity in many types of solid tumors (34). However, further studies are needed to clarify the detailed tumor suppressor function of HSPB7 in RCC.

The third important finding in this study is that HSPB7 was likely to be involved in the p53 pathway. The expression of HSPB7 was significantly induced in p53-dependent manner that was clearly demonstrated by two experiments, i) that introduction of adeno-p53 in p53-negative cancer cells showed strong induction of HSPB7 and ii) that DNA-damage-dependent introduction of HSPB7 was observed in HCT116 cells with wild-type p53, but not in those lacking p53. Although we failed to identify the p53-binding site in or near the HSPB7 gene, these two pieces of evidence strongly imply a critical role of HSPB7 as the direct/indirect p53-signal transducer and its downregulation may be involved in the development of various types of cancer including RCC.

In conclusion, we carried out a genome-wide gene expression analysis and identified HSPB7 to be a candidate tumor suppressor gene in RCC. We confirmed downregulation of this gene caused by DNA hypermethylation, its growth suppressive effect in RCC cell lines and its p53-dependent expression, indicating the important roles of HSPB7 in renal carcinogenesis. Our finding could contribute to better understanding of the novel function of HSPB7 in cancer.

Acknowledgements

We thank Ryuji Hamamoto, Daechun Kang and Takashi Fujitomo for technological support of IHC. We also thank Jinichi Mori for making cDNA template after Adriamycin treatment. We thank Satomi Takahashi for providing general reagents, materials and sequencing.

References

1. Ferlay J, Shin HR, Bray F, Forman D, Mathers C and Parkin DM: Estimates of worldwide burden of cancer in 2008: GLOBOCAN 2008. Int J Cancer 127: 2893-2917, 2010.
2. Jemal A, Bray F, Center MM, Ferlay J, Ward E and Forman D: Global cancer statistics. CA Cancer J Clin 61: 69-90, 2011.
3. Naito S, Tomita Y, Rha SY, *et al*: Kidney Cancer Working Group report. Jpn J Clin Oncol 40 (Suppl 1): i51-i56, 2010.
4. Siegel R, Naishadham D and Jemal A: Cancer statistics, 2012. CA Cancer J Clin 62: 10-29, 2012.
5. Chow WH, Devesa SS, Warren JL and Fraumeni JF Jr: Rising incidence of renal cell cancer in the United States. JAMA 281: 1628-1631, 1999.
6. Hock LM, Lynch J and Balaji KC: Increasing incidence of all stages of kidney cancer in the last 2 decades in the United States: An analysis of Surveillance, Epidemiology and End Results program data. J Urol 167: 57-60, 2002.
7. Lindblad P: Epidemiology of renal cell carcinoma. Scand J Surg 93: 88-96, 2004.
8. Murai M and Oya M: Renal cell carcinoma: etiology, incidence and epidemiology. Curr Opin Urol 14: 229-233, 2004.
9. Motzer RJ, Agarwal N, Beard C, *et al*: NCCN clinical practice guidelines in oncology: kidney cancer. J Natl Compr Canc Netw 7: 618-630, 2009.
10. Ljungberg B, Cowan NC, Hanbury DC, *et al*: EAU guidelines on renal cell carcinoma: the 2010 update. Eur Urol 58: 398-406, 2010.
11. Escudier B, Eisen T, Porta C, *et al*: Renal cell carcinoma: ESMO Clinical Practice Guidelines for diagnosis, treatment and follow-up. Ann Oncol 23 (Suppl 7): vii65-vii71, 2012.
12. Lam JS, Leppert JT, Belldegrun AS and Figlin RA: Novel approaches in the therapy of metastatic renal cell carcinoma. World J Urol 23: 202-212, 2005.
13. Cairns P: Renal cell carcinoma. Cancer Biomark 9: 461-473, 2010.
14. Molina AM and Motzer RJ: Current algorithms and prognostic factors in the treatment of metastatic renal cell carcinoma. Clin Genitourin Cancer 6 (Suppl 1): S7-S13, 2008.
15. Ono K, Tanaka T, Tsunoda T, *et al*: Identification by cDNA microarray of genes involved in ovarian carcinogenesis. Cancer Res 60: 5007-5011, 2000.
16. Hirota E, Yan L, Tsunoda T, *et al*: Genome-wide gene expression profiles of clear cell renal cell carcinoma: Identification of molecular targets for treatment of renal cell carcinoma. Int J Oncol 29: 799-827, 2006.
17. Saito-Hisaminato A, Katagiri T, Kakiuchi S, Nakamura T, Tsunoda T and Nakamura Y: Genome-wide profiling of gene expression in 29 normal human tissues with a cDNA microarray. DNA Res 9: 35-45, 2002.
18. Oda K, Arakawa H, Tanaka T, *et al*: p53AIP1, a potential mediator of p53-dependent apoptosis, and its regulation by Ser-46-phosphorylated p53. Cell 102: 849-862, 2000.
19. Matsuda K, Yoshida K, Taya Y, Nakamura K, Nakamura Y and Arakawa H: p53AIP1 regulates the mitochondrial apoptotic pathway. Cancer Res 62: 2883-2889, 2002.
20. Tanikawa C, Ueda K, Nakagawa H, Yoshida N, Nakamura Y and Matsuda K: Regulation of Protein Citrullination through p53/PAD14 Network in DNA Damage Response. Cancer Res 69: 8761-8769, 2009.
21. Tanikawa C, Matsuda K, Fukuda S, Nakamura Y and Arakawa H: p53RDL1 regulates p53-dependent apoptosis. Nat Cell Biol 5: 216-223, 2003.
22. Watanabe G, Kato S, Nakata H, Ishida T, Ohuchi N and Ishioka C: alphaB-crystallin: a novel p53-target gene required for p53-dependent apoptosis. Cancer Sci 100: 2368-2375, 2009.
23. Evans JR, Bosman JD, Brown-Endres L, Yehiely F and Cryns VL: Induction of the small heat shock protein alphaB-crystallin by genotoxic stress is mediated by p53 and p73. Breast Cancer Res Treat 122: 159-168, 2010.
24. Krief S, Faivre JF, Robert P, *et al*: Identification and characterization of cvHsp. A novel human small stress protein selectively expressed in cardiovascular and insulin-sensitive tissues. J Biol Chem 274: 36592-36600, 1999.
25. Sun X, Fontaine JM, Rest JS, Shelden EA, Welsh MJ and Benndorf R: Interaction of human HSP22 (HSPB8) with other small heat shock proteins. J Biol Chem 279: 2394-2402, 2004.
26. Vos MJ, Zijlstra MP, Kanon B, *et al*: HSPB7 is the most potent polyQ aggregation suppressor within the HSPB family of molecular chaperones. Hum Mol Genet 19: 4677-4693, 2010.
27. Cappola TP, Li M, He J, *et al*: Common variants in HSPB7 and FRMD4B associated with advanced heart failure. Circ Cardiovasc Genet 3: 147-154, 2010.
28. Matkovich SJ, Van Booven DJ, Hindes A, *et al*: Cardiac signaling genes exhibit unexpected sequence diversity in sporadic cardiomyopathy, revealing HSPB7 polymorphisms associated with disease. J Clin Invest 120: 280-289, 2010.
29. Stark K, Esslinger UB, Reinhard W, *et al*: Genetic association study identifies HSPB7 as a risk gene for idiopathic dilated cardiomyopathy. PLoS Genet 6: e1001167, 2010.
30. Villard E, Perret C, Gary F, *et al*: A genome-wide association study identifies two loci associated with heart failure due to dilated cardiomyopathy. Eur Heart J 32: 1065-1076, 2011.
31. Li XP, Luo R, Hua W and Hua W: Polymorphisms of Hspb7 gene associate with idiopathic dilated cardiomyopathy susceptibility in a Chinese population. Heart 98: E47-E47, 2012.
32. Rosenfeld GE, Mercer EJ, Mason CE and Evans T: Small heat shock proteins Hspb7 and Hspb12 regulate early steps of cardiac morphogenesis. Dev Biol 381: 389-400, 2013.
33. Huang Z, Cheng Y, Chiu PM, *et al*: Tumor suppressor Alpha B-crystallin (CRYAB) associates with the cadherin/catenin adherens junction and impairs NPC progression-associated properties. Oncogene 31: 3709-3720, 2012.
34. Ragnarsson G, Eiriksdottir G, Johannsdottir JT, Jonasson JG, Egilsson V and Ingvarsson S: Loss of heterozygosity at chromosome 1p in different solid human tumours: association with survival. Br J Cancer 79: 1468-1474, 1999.

Published OnlineFirst May 15, 2014; DOI: 10.1158/0008-5472.CAN-13-3037

Molecular and Cellular Pathobiology

Cancer Research

A Rare Polymorphic Variant of *NBS1* Reduces DNA Repair Activity and Elevates Chromosomal Instability

Yuki Yamamoto[1,2], Mamiko Miyamoto[1], Daisuke Tatsuda[1,4], Michiaki Kubo[5], Hitoshi Nakagama[1], Yusuke Nakamura[3], Hitoshi Satoh[2], Koichi Matsuda[3], Toshiki Watanabe[2], and Tsutomu Ohta[1]

Abstract

Failure to expeditiously repair DNA at sites of double-strand breaks (DSB) ultimately is an important etiologic factor in cancer development. NBS1 plays an important role in the cellular response to DSB damage. A rare polymorphic variant of *NBS1* that resulted in an isoleucine to valine substitution at amino acid position 171 (I171V) was first identified in childhood acute lymphoblastic leukemia. This polymorphic variant is located in the N-terminal region that interacts with other DNA repair factors. In earlier work, we had identified a remarkable number of structural chromosomal aberrations in a patient with pediatric aplastic anemia with a homozygous polymorphic variant of NBS1-I171V; however, it was unclear whether this variant affected DSB repair activity or chromosomal instability. In this report, we demonstrate that NBS1-I171V reduces DSB repair activity through a loss of association with the DNA repair factor MDC1. Furthermore, we found that heterozygosity in this polymorphic variant was associated with breast cancer risk. Finally, we showed that this variant exerted a dominant-negative effect on wild-type NBS1, attenuating DSB repair efficiency and elevating chromosomal instability. Our findings offer evidence that the failure of DNA repair leading to chromosomal instability has a causal impact on the risk of breast cancer development. *Cancer Res; 74(14); 3707–15. ©2014 AACR.*

Introduction

Nijmegen breakage syndrome, an autosomal recessive human disease, is because of a mutation in the *NBS1* gene (1). The clinical features of this syndrome include growth retardation, immunodeficiency, and increased susceptibility to malignancies (1). A gene product of the nibrin gene [*NBN*, also known as the Nijmegen breakage syndrome 1 gene (*NBS1*)] is a member of the MRE11/RAD50/NBS1 (MRN) protein complex, which is involved in the repair of double-strand break (DSB) in DNA (2). NBS1 consists of 2 functional regions (Fig. 1A). Its C-terminal region contains binding motifs of MRE11 meiotic recombination 11 homolog A (*Saccharomyces cerevisiae*; MRE11A, also known as MRE11) and ataxia telangiectasia–mutated (ATM) kinase (3–5), whereas its N-terminal region contains forkhead-associated (FHA) and breast cancer C-terminal (BRCT) domain that mediates phospho-dependent protein–protein interactions (6–8). A rare polymorphic variant of *NBS1* that resulted in an isoleucine to valine substitution at amino acid position 171 (I171V) was first identified in childhood acute lymphoblastic leukemia (ALL; ref. 9). The *NBS1*-I171V polymorphic variant is located in the BRCT domain, which is highly conserved in human, mouse, rat, chicken, and African clawed frog (Fig. 1B). We have previously described a patient with aplastic anemia (AA) in a Japanese child with a homozygous polymorphic variant of *NBS1*-I171V (10). We also determined that the chromosomes of lymphoblastic cell lines derived from this patient contained a remarkable number of structural chromosomal aberrations (10). However, it is unclear whether the *NBS1*-I171V polymorphic variant affects DSB repair activity and genomic instability.

In this study, we showed that NBS1-I171V decreased the localization of the MRN complex to sites of plural DSBs through its loss of association with MDC1. This aberrant localization resulted in decreased production of repairable single-stranded DNA and reduced DSB repair activity. We also showed that the heterozygous *NBS1*-I171V variant increased the risk of breast cancer in Japanese women. The NBS1-I171V reduced the DSB repair activity of endogenous NBS1 in a dominant-negative manner, and increased chromosomal instability.

Materials and Methods

Cell lines and antibodies

HeLa, HCC1937, GM07166VA7, GM07166VA7 transfected with DR-GFP reporter, and HS-SY-II cells were obtained from the American Type Culture Collection (ATCC), Dr. K. Komatsu (Kyoto University, Japan), and Dr. S. Sonobe (Kouchi Medical

Authors' Affiliations: [1]Division of Integrative Omics and Bioinformatics, National Cancer Center Research Institute; [2]Department of Medical Genome Sciences, Graduate School of Frontier Sciences; and [3]Human Genome Center Institute of Medical Science, The University of Tokyo; [4]Institute of Microbial Chemistry (BIKAKEN), Tokyo; and [5]Center for Genomic Medicine, The Institute of Physical and Chemical Research (RIKEN), Yokohama, Japan

Note: Supplementary data for this article are available at Cancer Research Online (http://cancerres.aacrjournals.org/).

Corresponding Author: Tsutomu Ohta, Division of Integrative Omics and Bioinformatics, National Cancer Center Research Institute, 5-1-1 Tsukiji Chuo-ku, Tokyo 104-0045, Japan. Phone: 81-3-3542-2511; Fax: 81-3-3248-1631; E-mail: cota@ncc.go.jp

doi: 10.1158/0008-5472.CAN-13-3037

Published OnlineFirst May 15, 2014; DOI: 10.1158/0008-5472.CAN-13-3037

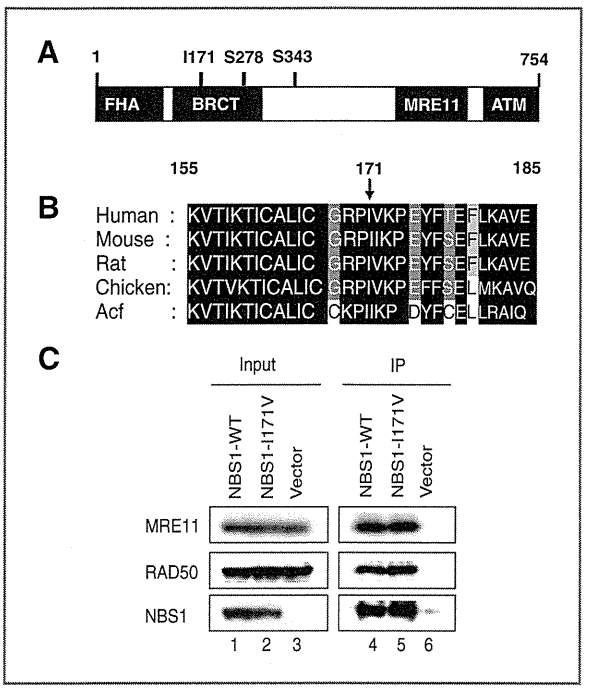

Figure 1. The polymorphic variant of *NBS1*-I171V is located in the BRCT domain. The structure of human NBS1 and the sequence alignment of the *NBS1*-I171V polymorphic variant region of various NBS1. A, NBS1 consists of functional regions: FHA and BRCT (BRCA1 C-terminus) domains at the N-terminus, MRE11, and ATM interacting motifs at the C-terminus, two ATM/ATR-phosphorylated serine residues (S278, S343). B, modified sequence alignment of the *NBS1*-I171V polymorphic variant region of various NBS1 from human, mouse, rat, chicken, and ACF (African clawed frog, *Xenopus laevis*). C, expression vectors containing 3xFlag-His-HA -NBS1-WT cDNA, -NBS1-I171V cDNA, or no cDNA (vector) were stably transfected into GM07166VA7 cells. Extracts from the cell lines were immunoprecipitated (IP) with anti-Flag antibody and then incubated with antibodies directed against MRE11, RAD50, or NBS1.

School, Japan), respectively. The following commercially available antibodies were used: mouse anti-Flag M2 monoclonal antibody (Sigma-Aldrich), rabbit anti-MDC1 antibody, mouse anti-MDC1 antibody, rabbit anti-p95 NBS1 antibody, rabbit anti-Mre11 antibody (Abcam), rabbit anti-phospho RPA32 (S4/S8) antibody (Bethyl Laboratories, Inc.), mouse anti-phospho histone H2AX (Ser139) antibody (Upstate), rabbit anti-RAD50 antibody, rabbit anti-RAD51 antibody (Santa Cruz Biotechnology, Inc.), and rabbit anti-BRCA1 antibody (Merck Millipore).

Plasmids and stable cell lines

The plasmids of pDRGFP and pCBASceI were obtained from addgene. The full-length human *NBS1* cDNA was a gift from Dr. Komatsu. The cDNA of *NBS1*-I171V or *NBS1*-wild-type (WT) with a 3xFlag-His6-HA-tag at C-terminus was generated by using PCR and then ligated into the pEB-Multi-Neo mammalian expression vector (Wako). These vectors were transfected into GM07166VA7 cells, GM07166VA7 cells containing DR-GFP reporter, and HeLa cells. The cells were cultured in the presence of 800 or 600 μg/mL G418 (Calbiochem) for 2 weeks, after which clones were isolated and selected on the basis of their NBS1 expression, with the selected clones expressing equivalent levels of protein.

Immunoprecipitation and immunofluorescence analyses

For immunoprecipitation analysis, the cells were washed with phosphate-buffered saline (PBS) and sonicated in lysis buffer [150 mmol/L NaCl, 20 mmol/L Tris-HCl (pH 7.9), 20% glycerol, and 1 mmol/L Pefabloc (a protease inhibitor; Roche)]. The lysate (1 mg) was mixed with anti-Flag M2 Affinity Gel (Sigma-Aldrich) and incubated for 4 hours at 4°C. The gel was washed three times with lysis buffer. The immunoprecipitated proteins were separated by using sodium dodecyl sulfate-polyacrylamide gel electrophoresis (SDS-PAGE) and then incubated with the indicated antibodies. For immunofluorescence analysis, the cells were cultured on glass coverslips, exposed to 10 Gy of ionizing radiation (IR). After 4 hours, the cells were fixed in ice-cold 4% paraformaldehyde for 1 hour, permeabilized with 0.1% TritonX-100 at room temperature, immersed in blocking reagent [2% normal swine serum (Funakoshi Inc.), 0.05% TritonX-100] for 30 minutes at room temperature, and then incubated with the indicated primary antibodies overnight at 4°C. The cells were incubated with secondary antibodies conjugated to Alexa Fluor 488 or Alexa Fluor 555 (Invitrogen) for 1 hour at room temperature and stained with 2 μg/mL of 4′,6-diamidino-2-phenylindole dihydrochloride (DAPI) for 10 minutes at room temperature. Images were captured with a confocal laser microscope (Carl Zeiss) with a ×40 water immersion objective.

DR-GFP assay

Homologous recombination (HR) repair frequency in the cell lines using DR-GFP system was performed as described previously (11, 12).

Cell-cycle assay

An appropriate number of cells was plated and then exposed to 10 Gy of IR. After 6 hours, the cell-cycle phase in the cells was analyzed by the Cell-Clock Mammalian Cell Cycle Assay Kit (biocolor life science assays).

Cell survival assay

An appropriate number of cells was plated and then exposed to IR, mitomycin C (MMC), or a poly-(ADP-ribose) polymerase 1 (PARP1) inhibitor (AZD2281). After 10 days of incubation, the surviving fractions were calculated by counting the number of colonies.

Small interfering RNA analysis

For the small interfering RNA (siRNA) experiments, the siRNA for control (4390844; Life Technologies), MDC1 (s18578; Life Technologies), and NBS1 (s9291 and s9292; Life Technologies) were used. Transfection was performed as described previously (13).

Cytogenetic analysis

After exposure to IR, the cells were cultured for 3 days and then treated with colcemid (0.02 μg/mL) for 2 hours before

Published OnlineFirst May 15, 2014; DOI: 10.1158/0008-5472.CAN-13-3037

being harvested. Chromosome slides were prepared by using standard protocols and then stained with a 5% Giemsa solution (Wako) for 30 minutes. For each cell line, about 1,600 well-spread metaphase chromosomes were screened for structural chromosomal aberrations.

Sample collection, genotyping, and statistical analysis

We obtained DNA samples of 1,524 breast cancer cases and 1,462 controls from the BioBank Japan Project as described previously (PMID: 22951594). As part of this project, patients' DNA samples were collected through a collaborative network of 66 hospitals throughout Japan. A list of participating hospitals can be found at the following website: http://biobankjp.org/plan/member_hospital.html. Genotyping of the *NBS1* variations at amino acid position 171 was performed by direct sequencing. The primers used for amplification were as follows: forward, 5′-TGGATGTAAACAGCCTCTTTGT-3′; reverse, 5′-TGAAACAAGCATTAAAGAGGGAA-3′. The odds ratios (OR) were calculated in a dominant mode. *P* values were calculated by using the χ^2 test.

Results and Discussions

NBS1-I171V polymorphic variant reduced DSB repair activity

To explore the biological consequences of the NBS1-I171V substitution, we generate cell lines that express the polymorphic variants of the *NBS1* gene. First, we constructed the *NBS1* cDNA to construct expression vectors that encoded a protein with either isoleucine (NBS1-WT) or valine (NBS1-I171V) at amino acid position 171. The vectors were stably transfected into human GM07166VA7 cells, which contain homozygous for the 657del5 mutation in exon 6. The mutation of NBS1 determines the synthesis of two truncated proteins of 26 kDa (p26) and 70 kDa (p70) (14). We isolated and selected clones with equivalent levels of NBS1 expression for further analysis (Fig. 1C, lanes 1 and 2, and Supplementary Fig. S1A). Immunoprecipitation analysis in these cloned cell lines indicated that both NBS1-I171V and NBS1-WT bound to MRE11 and RAD50 homolog (*S. cerevisiae*; RAD50; Fig. 1C, lanes 4 and 5), suggesting that NBS1-I171V can incorporate into the MRN protein complex. We also used these NBS1-expressing cell lines to assess cell survival in response to DNA damage caused by IR or the cross-linking agent MMC. An analysis of cell survival revealed that the cell line expressing NBS1-I171V was more sensitive to IR and MMC than was the cell line expressing NBS1-WT (Fig. 2A). We also found that other cell line expressing NBS1-I171V was more sensitive to IR and MMC than was other cell line expressing NBS1-WT (Supplementary Fig. S1B). Next, we analyzed HR repair frequency in the NBS1-expressing cell lines with DR-GFP system (11, 12). When I-*Sce*I expression was induced, the cell line expressing NBS1-I171V showed a 3-fold lower frequency in HR repair compared with the cell line expressing NBS1-WT (Fig. 2B). We also found that other cell line expressing NBS1-I171V showed lower frequency in HR repair compared with other cell line expressing NBS1-WT (Supplementary Fig. S1C). It was reported that a PARP1 inhibitor (AZD2281) reduced growth of HR repair–deficient cells such as *BRCA1* and *BRCA2* mutated cells (15, 16). Therefore, we examined cell survival in response to AZD2281. We found that the cell line expressing NBS1-I171V was more sensitive to AZD2281 than was the cell line expressing NBS1-WT, but was more resistant to AZD2281 than was the cell line expressing a vector (Fig. 2C and Supplementary Fig. S2A). This result indicated that damages

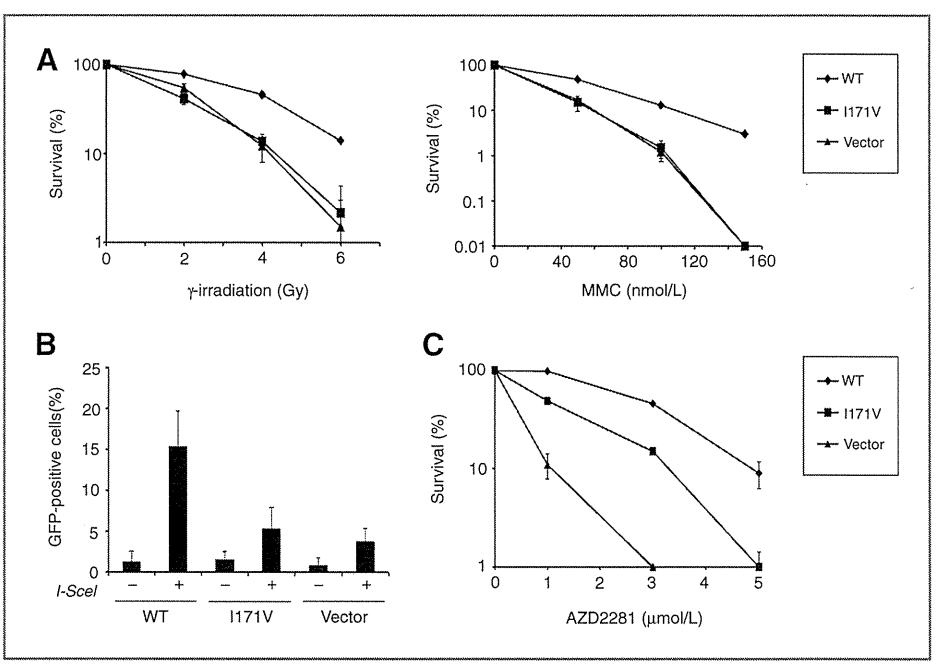

Figure 2. Reduced DSB repair activity in cells expressing an *NBS1-I171V* polymorphic variant. A, the survival of the GM07166VA7 cell lines expressing NBS1-WT (WT), NBS1-I171V (I171V), or the vector (vector) were analyzed by using a colony formation assay after exposure to 0, 2, 4, or 6 Gy of IR or 0, 50, 100, or 150 nmol/L of MMC. Data, mean ± SEM ($n = 3$). B, HR repair activity in the GM07166VA7 cell lines expressing NBS1-WT (WT), NBS1-I171V (I171V), or the vector (vector) was measured with the DR-GFP assay. Data, mean ± SEM ($n = 3$). C, the survival of the GM07166VA7 cell lines expressing NBS1-WT (WT), NBS1-I171V (I171V), or the vector were analyzed by using a colony formation assay after exposure to 0, 1, 3, or 5 μmol/L of AZD2281. Data, mean ± SEM ($n = 3$).

Published OnlineFirst May 15, 2014; DOI: 10.1158/0008-5472.CAN-13-3037

by the PARP inhibitor were different from those by IR or MMC in Fig. 2A. We showed that HR repair activity of GM07166VA7 cells expressing NBS1-I171V was almost similar to that of GM07166VA7 cells expressing a vector in Fig. 2B. These results suggested that damages by the PARP inhibitor were repaired by HR repair–dependent and –independent manners of NBS1. We speculate that NBS1-I171V has the HR repair–independent activity to repair damages by the PARP inhibitor. However, the activity of NBS1-I171V is still unclear. Thus, further research of NBS1-I171V function could be necessary.

It was reported that NBS cells exposed to IR showed an abnormal cell cycle (17). Therefore, we examined the cell-cycle status of the cells that had been exposed to IR. We found that the ratio of S phase in the cell expressing the NBS1-WT was reduced by IR treatment, but not in the cell expressing the NBS1-I171V or the vector (Supplementary Fig. S2B). This result suggests that G_1–S phase arrest is failed in cells expressing NBS1-I171V. These results suggest that the DSB repair activity of cells expressing NBS1-I171V is reduced compared with that of cells expressing NBS1-WT and prompted a more in-depth analysis of these cell lines.

NBS1-I171V polymorphic variant decreased the localization of the MRN complex to sites of DSB

NBS1 is known to be involved in an early step of DSB repair (2). Thus, we used immunofluorescence to examine whether NBS1-I171V localizes to sites of DSB in cells exposed to IR. We observed NBS1 foci in cells expressing NBS1-WT, but not in those expressing NBS1-I171V (Fig. 3A and B). MRE11 foci were also identified in cells expressing NBS1-WT, but not in those expressing NBS1-I171V (Fig. 3C and D). Phosphorylated H2A histone family member X (γH2AX) foci were identified in both the cells expressing

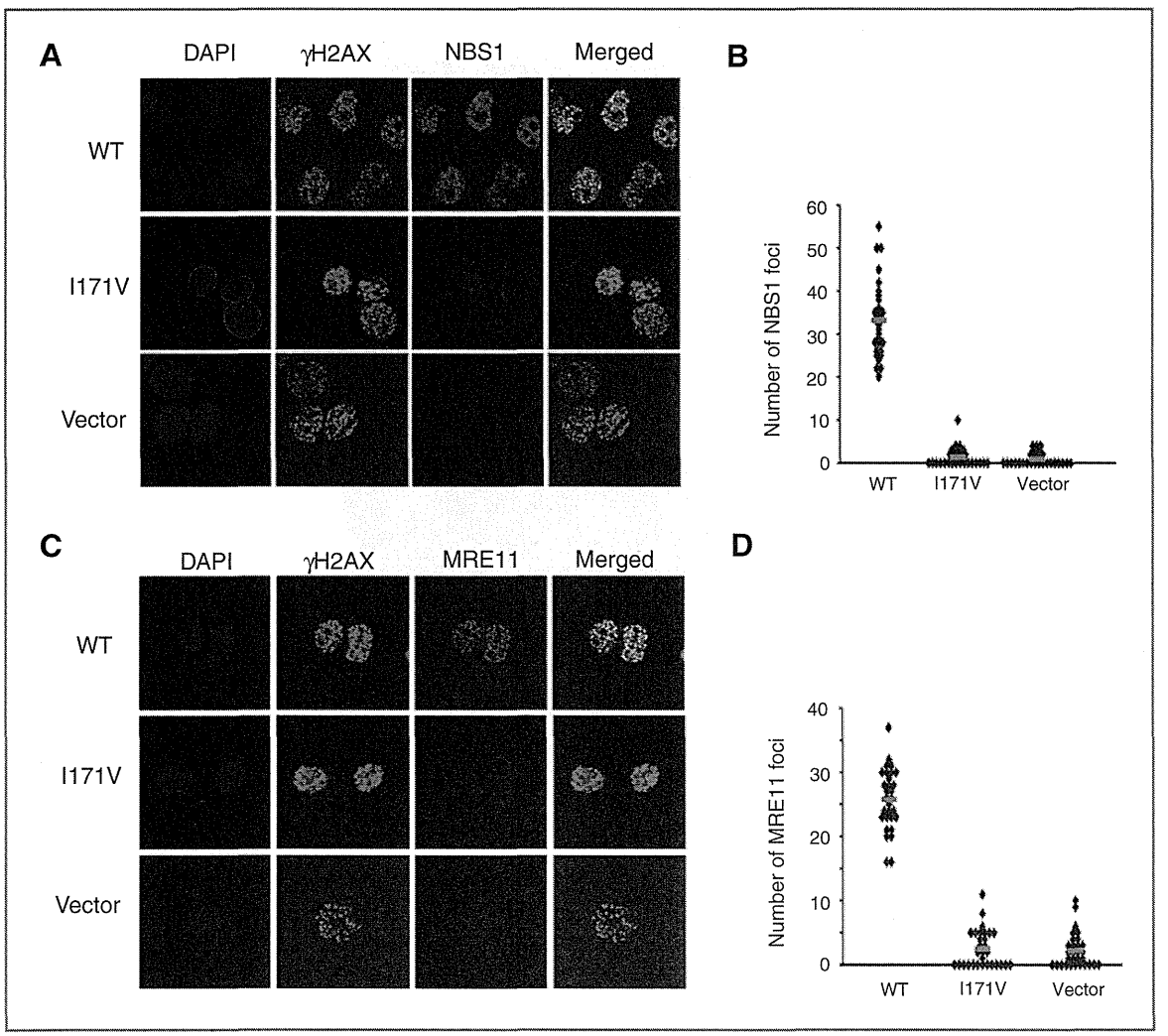

Figure 3. Reduced localization of NBS1 and MRE11 at the DSB sites in cells expressing an *NBS1-I171V* polymorphic variant. A and C, focus formation of NBS1, MRE11, and γH2AX. The GM07166VA7 cells expressing NBS1-WT (WT), NBS1-I171V (I171V), and the vector were irradiated with 10 Gy of IR. After 4 hours, the cells were incubated with antibodies directed against NBS1, γH2AX, or MRE11 and then stained with DAPI. B and D, scatter plots of NBS1 or MRE11 focus counts per cell in Fig. 3A or C are shown ($n = 30$). Red bars, median.

Published OnlineFirst May 15, 2014; DOI: 10.1158/0008-5472.CAN-13-3037

NBS1-I171V and those expressing NBS1-WT, where they colocalized with the NBS1-WT foci or MRE11 foci (Fig. 3). These results suggest that after exposure to IR, the localization of NBS1-I171V to sites of DSB is less prominent than that of NBS1-WT.

NBS1-I171V polymorphic variant reduced DSB repair activity through loss of association with MDC1

Because mediator of DNA-damage checkpoint 1 (MDC1) recruits NBS1 to sites of DSB after IR treatment (18, 19), we examined MDC1 localization in cells that had been exposed to IR. MDC1 foci were identified at sites of DSB in cells expressing either NBS1-I171V or NBS1-WT (Fig. 4A and B). These results suggest that MDC1's ability to localize to sites of DSB after IR treatment is unaffected by the NBS1-I171V substitution. We also determined that MDC1 foci localized at sites of DSB with NBS1-WT foci but not with NBS1-I171V foci after IR treatment (Fig. 4C and D). Next, we characterized the interaction between NBS1-I171V and MDC1 by conducting an immunoprecipitation analysis. After exposure to IR, a large amount of MDC1 coprecipitated with NBS1-WT, but not with NBS1-I171V (Fig. 4E, lanes 4 and 5). This result is consistent with the reports that both of FHA and BRCT domains in NBS1 are important for its association with MDC1 (8, 20), and NBS1-K160M mutant that resulted in an lysine to methionine substitution at amino acid position 160 within the BRCT domain reduces its binding activity to MDC1 (8). Therefore, we speculate that NBS1-I171V mutant within the BRCT domain affects a structure of the BRCT domain and abolishes the interaction between NBS1 and MDC1. The results in Fig. 4 suggest that the decreased localization of NBS1-I171V to sites of IR-induced DSB results

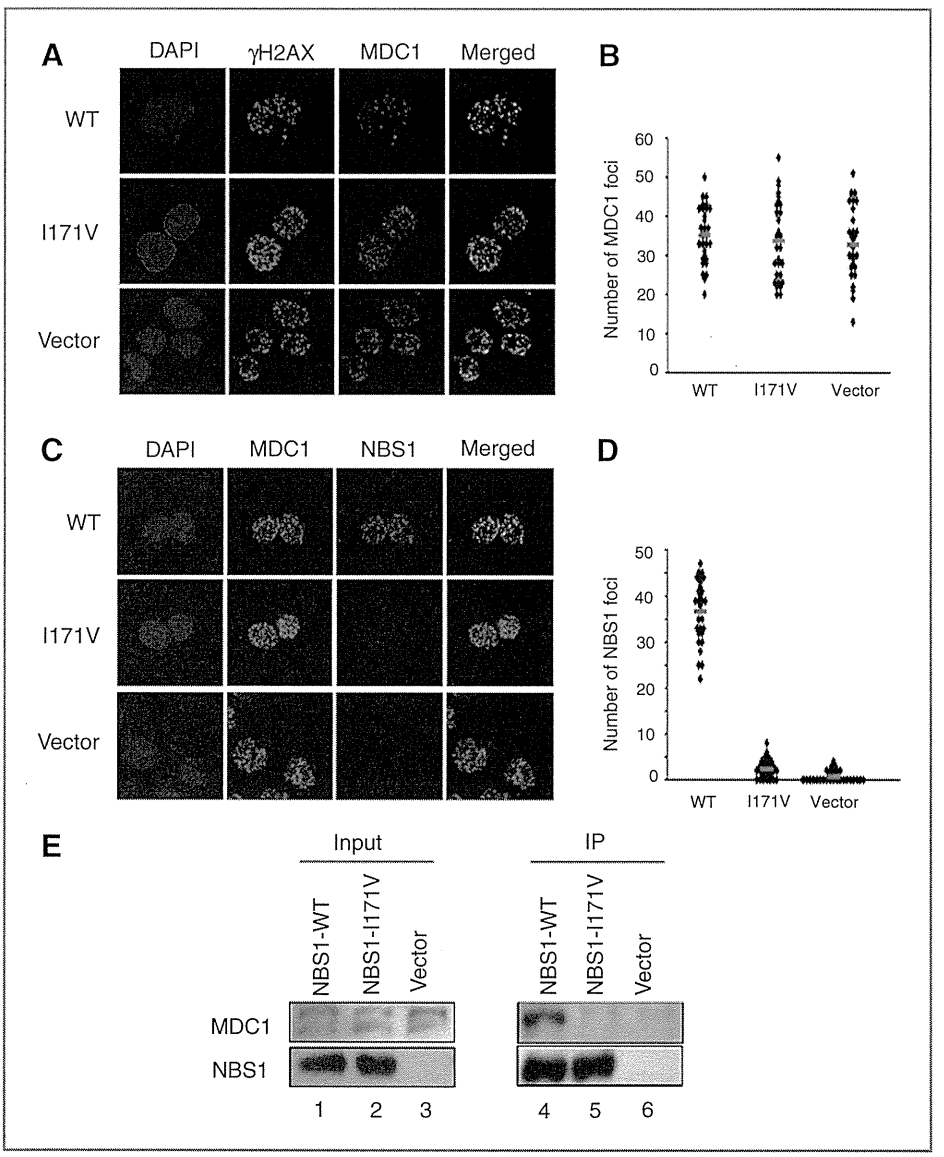

Figure 4. Reduced association of the NBS1-I171V polymorphic variant with MDC1. A and C, focus formation of γH2AX, MDC1, and NBS1. The GM07166VA7 cells expressing NBS1-WT (WT), NBS1-I171V (I171V), and the vector were irradiated with 10 Gy of IR. After 4 hours, the cells were incubated with antibodies directed against γH2AX, MDC1, or NBS1 and then stained with DAPI. B and D, scatter plots of MDC1 or NBS1 focus counts per cell in Fig. 4A or C are shown ($n = 30$). Red bars, median. E, the GM07166VA7 cells expressing NBS1-WT, NBS1-I171V, and the vector were irradiated with 10 Gy of IR. After 4 hours, whole cell lysates were prepared. The cell lysates were immunoprecipitated with anti-Flag antibody and then incubated with antibodies directed against MDC1 or NBS1.

Published OnlineFirst May 15, 2014; DOI: 10.1158/0008-5472.CAN-13-3037

from its inability to bind to MDC1. We also found that the knockdown of MDC1 expression using MDC1-specific siRNA did not affect the sensitivity to IR in cell line expressing NBS1-I171V or the vector (Supplementary Fig. S3A). However, the knockdown of MDC1 expression increased the sensitivity to IR in cell line expressing NBS1-WT (Supplementary Fig. S3A). This result suggests that NBS1-I171V impairs the MDC1–NBS1 pathway.

The MRN complex initiates resection of DSB ends to create single-stranded 3′-overhangs that can be repaired by HR system (21). In addition, the complex recruits replication protein A (RPA), containing phosphorylated 32 kDa replication protein A2 subunit (RPA2, also known as RPA32), to single-stranded DNA at sites of DSB (22). We examined the production of single-stranded DNA at the ends of DSB by using immunofluorescence to analyze the localization of phosphorylated RPA32 in cells exposed to IR. Phosphorylated RPA32 foci were identified at sites of DSB in cells expressing NBS1-WT, but not in those expressing NBS1-I171V or the vector control (Fig. 5A and B). Because RAD51 homolog (*S. cerevisiae*; RAD51) also was recruited to the single-stranded 3′-overhangs after IR treatment (23), we examined RAD51 localization in cells that had been exposed to IR. RAD51 foci were identified at sites of DSB in cells expressing NBS1-WT, but not in those expressing NBS1-I171V or the vector (Fig. 5C and D). It was reported that BRCA1 (familial breast cancer susceptibility protein) also promoted induction of the single-stranded DNAs at sites of DSB (24). Therefore, we examined BRCA1 localization in cells that had been exposed to IR. BRCA1 foci were identified at sites of DSB in cells expressing NBS1-WT, but not in cells expressing NBS1-I171V or the vector (Supplementary Fig. S3C and S3D). These results are consistent with our finding that the localization of NBS1-I171V to sites of IR-induced DSB was less pronounced than that of NBS1-WT (Fig. 3A and B), and suggest that NBS1-I171V decreases the localizations of the MRN complex and BRCA1 to sites of DSB. These aberrant localizations result in decreased production of repairable single-stranded DNA and reduced DSB repair activity.

NBS1-I171V polymorphic variant increases the risk of breast cancer

To date, the *NBS1*-I171V polymorphic variant was detected frequently only in Polish patients with breast cancer, head and neck cancer, and colorectal cancer (25–28). However, other groups did not find a similar association in European patients with breast cancer, leukemia, or lymphoma (29–31). It remains unclear whether this particular polymorphic variant of the *NBS1* gene is associated with cancer. It was reported that although null mutations in the mouse *NBS1* gene resulted in embryonic lethality at the

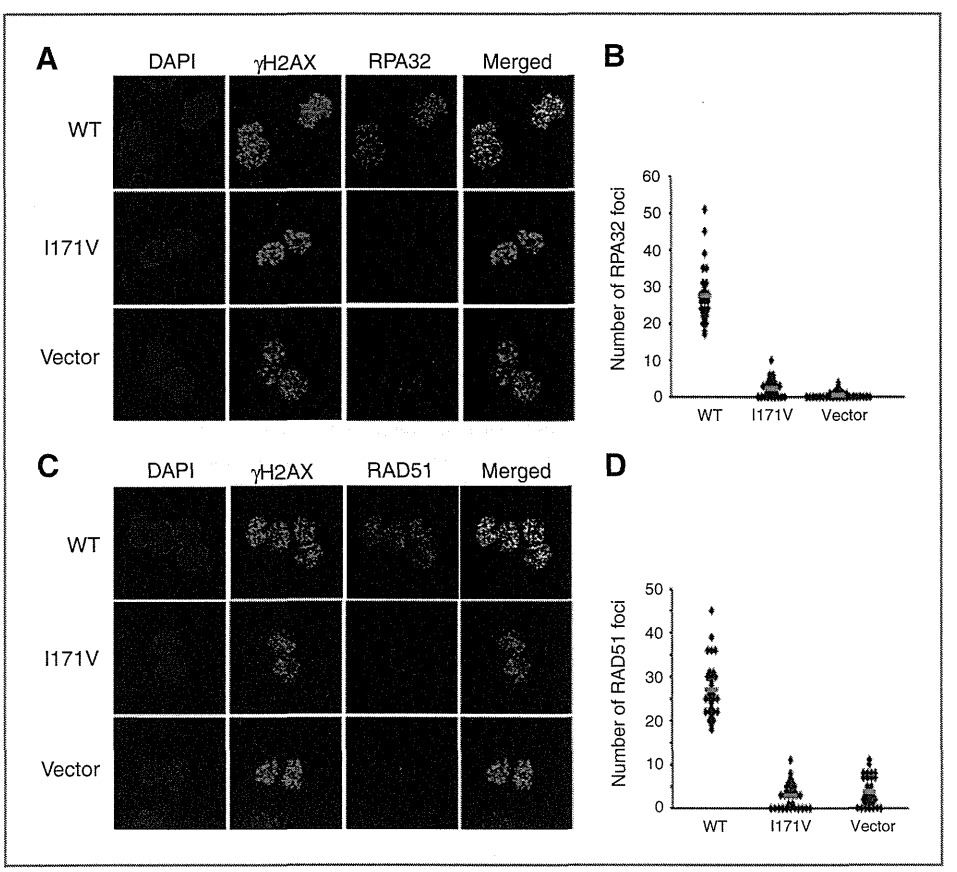

Figure 5. Reduced association of RPA32 and RAD51 at the DSB sites in cells expressing an *NBS1-I171V* polymorphic variant. A and C, focus formation of γH2AX, phospho-RPA32, and RAD51. The GM07166VA7 cells expressing NBS1-WT (WT), NBS1-I171V (I171V), and the vector were irradiated with 10 Gy of IR. After 4 hours, the cells were incubated with antibodies directed against γH2AX, phospho-RPA32, or RAD51 and then stained with DAPI. B and D, scatter plots of phospho-RPA32 or RAD51 focus counts per cell in Fig. 5A or C are shown ($n = 30$). Red bars, median.

Published OnlineFirst May 15, 2014; DOI: 10.1158/0008-5472.CAN-13-3037

Table 1. Association of *NBS1* variation with breast cancer in Japanese

SNP Gene	Allele 1/2[a]	Groups	Case 11	Case 12	Case 22	RAF	P^b	OR[c] (95% CI)
rs61754966	G/A	Breast	0	23	1,501	0.0075	0.0048	3.19 (1.36–7.44)
NBS1		Control	0	7	1,455	0.0024		

NOTE: We analyzed 1,524 breast cancers and 1,462 controls.
[a]Allele 1, risk allele; Allele 2, nonrisk allele.
[b]*P* value and [c]OR were calculated in a dominant model (11 + 12 vs. 22).

blastocyst stage, heterozygous knockout ($NBS1^{+/-}$) mice developed a wide array of tumors (32). Moreover, cell-cycle–dependent association of BRCA1 with the MRN protein complex contributes to the activation of HR-mediated DSB repair in S and G_2 phases of the cell cycle (33). These reports strongly suggest that the *NBS1*-I171V polymorphic variant may increase breast cancer risk. Therefore, we analyzed the association of the *NBS1*-I171V variant with breast cancer in a Japanese population; patient characteristics are presented in Supplementary Table S1. Of the 1,524 Japanese women with cancer, 23 (1.6%) carried the heterozygous polymorphic variant. Only 7 women (0.48%) with the heterozygous polymorphic variant were found in the control group ($n = 1{,}462$). None of the patients in the breast cancer group or in the control group carried the homozygous polymorphic variant of the *NBS1*-I171V substitution. The frequency of patients with the heterozygous *NBS1* polymorphic variant in the Japanese breast cancer group [OR, 3.19; 95% confidence interval (CI), 1.36–7.44; $P = 0.0048$] was significantly higher than that in the control group (Table 1). This result suggests that the *NBS1*-I171V variant increases the risk of breast cancer in Japanese women.

NBS1-I171V polymorphic variant elevated chromosomal instability

The above finding may suggest that NBS1-I171V exerts a dominant-negative effect on the function of NBS1-WT. To test this hypothesis, we expressed the codon 171 polymorphic variants of NBS1 in HeLa cells, which also express endogenous NBS1. Clones were isolated and selected on the basis of their exogenous and endogenous NBS1 expression, with the selected clones expressing equivalent levels of protein (Fig. 6A, lanes 1 and 2). Using these cell lines, we assessed cell survival in response to DNA damage caused by exposure to IR or MMC. The cell line expressing NBS1-I171V was more sensitive to IR and MMC than was the line expressing NBS1-WT or the vector (Fig. 6B). We also found that other cell line expressing NBS1-I171V was more sensitive to IR and MMC than was other cell line expressing NBS1-WT (Supplementary Fig. S4B). Next, we analyzed the localization of NBS1, MRE11, phosphorylated RPA32, RAD51, or BRCA1 in cells exposed to IR. The cell line expressing NBS1-I171V showed a 2- to 3-fold lower focus counts of NBS1, MRE11, phosphorylated RPA32, RAD51, or BRCA1 compared with the cell line expressing NBS1-WT or the vector (Supplementary Figs. S4D, S4E, S5, S6, and S7). These results suggest that the DSB repair activity of endogenous NBS1 was reduced by NBS1-I171V in a dominant-negative manner. Figure 6A showed that total amount of NBS1 protein in HeLa cell line expressing NBS1-I171V or NBS1-WT was almost same as that in HeLa cell line expressing a vector. Because NBS1-I171V incorporates into the MRN protein complex (Fig. 1C), the half of the MRN protein complex contains NBS1-I171V in HeLa cell line expressing NBS1-I171V. Therefore, we think that decreased the amount of MRN protein complex containing wild-type NBS1 in HeLa cell line expressing NBS1-I171V shows the dominant negative effect in response to DNA damage caused by exposure to IR or MMC.

We also assessed the structural aberrations of the chromosomes in each cell line after exposure to IR and discovered that the number of aberrations in the cell line expressing NBS1-I171V [28 double minutes (DM), 7 chromatid gaps (CTG), and 8 chromatid breaks (CTB)/~1,600 chromosomes; a representative metaphase spread is shown in Fig. 6C] was significantly higher than that of cell line expressing either NBS1-WT or the vector control (NBS1-WT: 4 DMs and 4 CTGs, vector control: 4 DMs, 1 CTG, and 1 CTB; both/~1,600 chromosomes; Fig. 6D). We also found that the number of aberrations in other cell line expressing NBS1-I171V was significantly higher than that of other cell line expressing either NBS1-WT or the vector control (Supplementary Fig. S8). These results suggest that chromosomal instability is elevated in cells expressing NBS1-I171V because its dominant-negative effects on endogenous NBS1 reduce DSB repair. This result is consistent with our previous finding that the chromosomes of lymphoblastic cell lines derived from the patient's father, who carried the heterozygous polymorphic variant of the *NBS1*-I171V substitution, contained a remarkable number of structural chromosomal aberrations (10).

Conclusion

We have demonstrated that the NBS1-I171V variant reduces DSB repair activity through loss of association with MDC1. Moreover, the reduced activity of NBS1 in cells expressing the NBS1-I171V variant elevated chromosomal instability in these cells and increased the risk of breast cancer in a

Published OnlineFirst May 15, 2014; DOI: 10.1158/0008-5472.CAN-13-3037

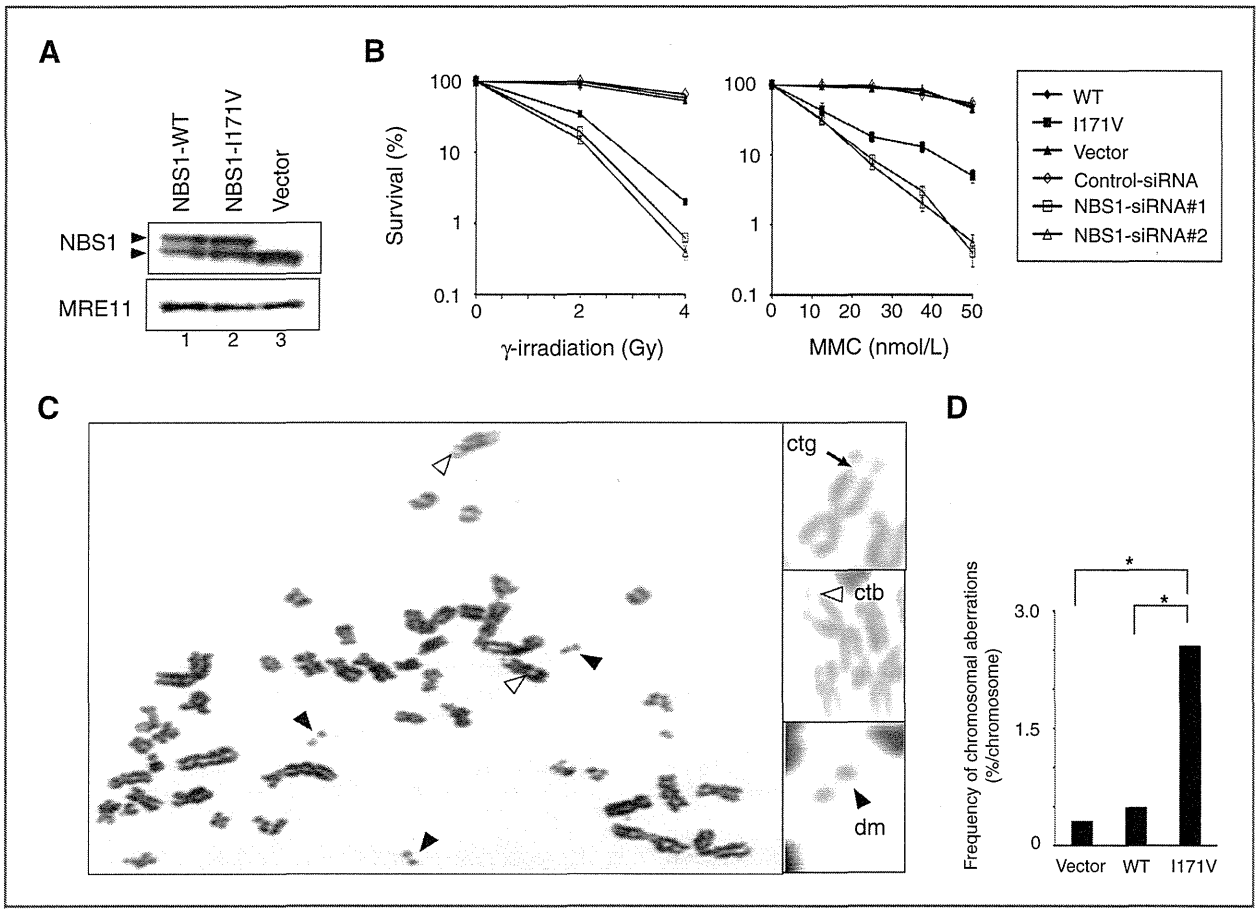

Figure 6. The DSB repair activity of endogenous NBS1 was repressed by the NBS1-I171V polymorphic variant in a dominant-negative manner. Expression vectors containing 3xFlag-His-HA-NBS1-WT cDNA, -NBS1-I171V cDNA, or no cDNA were stably transfected into HeLa cells. A, the expression levels of NBS1 in the cell extracts were analyzed with antibodies directed against NBS1. The upper arrowhead indicates exogenous NBS1 and the lower arrowhead indicates endogenous NBS1. B, the survival of the cell lines expressing NBS1-WT (WT), NBS1-I171V (I171V) or the vector, or the survival of HeLa cells transfected with NBS1 siRNA (NBS1-siRNA#1 and siRNA#2) or control siRNA (control-siRNA) was analyzed by using colony formation assays after exposure to 0, 2, or 4 Gy of IR or 0, 12.5, 25, 37.5, or 50 nmol/L of MMC. Data, mean ± SEM ($n = 3$). C, a representative metaphase spread of the HeLa cells expressing NBS1-I171V after exposure to 6 Gy of IR. CTBs (white arrowheads), DMs (black arrowheads), and CTGs (arrows) are indicated. Noteworthy, structural chromosomal aberrations are shown at higher magnification in the right panels: CTG (top), CTB (middle), and DM (bottom). D, comparison of the frequencies of aberrations found in the cells used in A. *, $P < 0.005$.

Japanese population. Recently, it was reported that Mre11-mediated DDR restrains mammary hyperplasia by effecting an oncogene-induced G_2 arrest (34). Therefore, further research of NBS1-I171V function in the development of breast cancer could be necessary.

Disclosure of Potential Conflicts of Interest

No potential conflicts of interest were disclosed.

Authors' Contributions

Conception and design: Y. Yamamoto, T. Ohta
Development of methodology: Y. Yamamoto
Acquisition of data (provided animals, acquired and managed patients, provided facilities, etc.): Y. Yamamoto, M. Miyamoto, D. Tatsuda, M. Kubo, K. Matsuda, T. Watanabe
Analysis and interpretation of data (e.g., statistical analysis, biostatistics, computational analysis): Y. Yamamoto, Y. Nakamura
Writing, review, and/or revision of the manuscript: Y. Yamamoto, H. Satoh, T. Watanabe, T. Ohta
Administrative, technical, or material support (i.e., reporting or organizing data, constructing databases): M. Kubo, H. Satoh, T. Watanabe
Study supervision: H. Nakagama, Y. Nakamura

Acknowledgments

The authors thank Dr. K. Komatsu (Kyoto University, Japan) for the *NBS1* cDNA, GM07166VA7 cells, and GM07166VA7 cells transfected with DR-GFP reporter, and Dr. M. Jasin (Sloan Kettering Cancer Center, USA) for the DR-GFP construct.

Grant Support

This work was supported in part by the National Cancer Center Research and Development Fund (23-A-4), and Grants-in-Aid for Cancer Research from the Ministry of Health, Labor, and Welfare of Japan. This work was also conducted as part of the BioBank Japan Project, which was supported by the Ministry of Education, Culture, Sports, Science, and Technology of Japan.

The costs of publication of this article were defrayed in part by the payment of page charges. This article must therefore be hereby marked *advertisement* in accordance with 18 U.S.C. Section 1734 solely to indicate this fact.

Received October 24, 2013; revised April 14, 2014; accepted April 29, 2014; published OnlineFirst May 15, 2014.

Published OnlineFirst May 15, 2014; DOI: 10.1158/0008-5472.CAN-13-3037

References

1. Weemaes CM, Hustinx TW, Scheres JM, van Munster PJ, Bakkeren JA, Taalman RD. A new chromosomal instability disorder: the Nijmegen breakage syndrome. Acta Paediatr Scand 1981;70:557–64.
2. Carney JP, Maser RS, Olivares H, Davis EM, Le Beau M, Yates JR 3rd, et al. The hMre11/hRad50 protein complex and Nijmegen breakage syndrome: linkage of double-strand break repair to the cellular DNA damage response. Cell 1998;93:477–86.
3. Desai-Mehta A, Cerosaletti KM, Concannon P. Distinct functional domains of nibrin mediate Mre11 binding, focus formation, and nuclear localization. Mol Cell Biol 2001;21:2184–91.
4. Falck J, Coates J, Jackson SP. Conserved modes of recruitment of ATM, ATR and DNA-PKcs to sites of DNA damage. Nature 2005;434:605–11.
5. You Z, Chahwan C, Bailis J, Hunter T, Russell P. ATM activation and its recruitment to damaged DNA require binding to the C terminus of Nbs1. Mol Cell Biol 2005;25:5363–79.
6. Kobayashi J, Tauchi H, Sakamoto S, Nakamura A, Morishima K, Matsuura S, et al. NBS1 localizes to γ-H2AX foci through interaction with the FHA/BRCT domain. Curr Biol 2002;12:1846–51.
7. Chapman JR, Jackson SP. Phospho-dependent interactions between NBS1 and MDC1 mediate chromatin retention of the MRN complex at sites of DNA damage. EMBO Rep 2008;9:795–801.
8. Lloyd J, Chapman JR, Clapperton JA, Haire LF, Hartsuiker E, Li J, et al. A supramodular FHA/BRCT-repeat architecture mediates Nbs1 adaptor function in response to DNA damage. Cell 2009;139:100–11.
9. Varon R, Reis A, Henze G, von Einsiedel HG, Sperling K, Seeger K. Mutations in the nijmegen breakage syndrome gene (NBS1) in childhood acute lymphoblastic leukemia (ALL). Cancer Res 2001; 61:3570–2.
10. Shimada H, Shimizu K, Mimaki S, Sakiyama T, Mori T, Shimasaki N, et al. First case of aplastic anemia in a Japanese child with a homozygous missense mutation in the NBS1 gene (I171V) associated with genomic instability. Hum Genet 2004;115:372–6.
11. Pierce AJ, Johnson RD, Thompson LH, Jasin M. XRCC3 promotes homology-directed repair of DNA damage in mammalian cells. Genes Dev 1999;13:2633–8.
12. Sakamoto S, Iijima K, Mochizuki D, Nakamura K, Teshigawara K, Kobayashi J, et al. Homologous recombination repair is regulated by domains at the N- and C-terminus of NBS1 and is dissociated with ATM functions. Oncogene 2007;26:6002–9.
13. Ishida M, Miyamoto M, Naitoh S, Tatsuda D, Hasegawa T, Nemoto T, et al. The SYT-SSX fusion protein down-regulates the cell proliferation regulator COM1 in t(x;18) synovial sarcoma. Mol Cell Biol 2007; 27:1348–55.
14. Master RS, Zinkel M, Petrini JHJ. An alternative mode of translation permits production of a variant NBS1 protein from the common Nijmegenbreakage syndrome allele. Nat Genet 2001;27:417–21.
15. Bryant HE, Schultz N, Thomas HD, Parker KM, Flower D, Lopez E, et al. Specific killing of BRCA2-deficient tumours with inhibitors of poly (ADP-ribose) polymerase. Nature 2005;434:913–7.
16. Farmer H, McCabe N, Lord CJ, Tutt AN, Johnson DA, Richardson TB, et al. Targeting the DNA repair defect in BRCA mutant cells as a therapeutic strategy. Nature 2005;434:917–21.
17. Jongmans W, Vuillaume M, Chrzanowska K, Smeets D, Sperling K, Hall J. Nijmegen breakage syndrome cells fail to induce the p53-mediated DNA damage response following exposure to ionizing radiation. Mol Cell Biol 1997;17:5016–22.
18. Goldberg M, Stucki M, Falck J, D'Amours D, Rahman D, Pappin D, et al. MDC1 is required for the intra-S-phase DNA damage checkpoint. Nature 2003;421:952–6.
19. Stewart GS, Wang B, Bignell CR, Taylor AM, Elledge SJ. MDC1 is a mediator of the mammalian DNA damage checkpoint. Nature 2003;421:961–6.
20. Williams SR, Dodson EG, Limbo O, Yamada Y, Williams SJ, Guenther G, et al. Nbs1 Flexibly tethers Ctp1 and Mre11-Rad50 to coordinate DNA double-strand break processing and repair. Cell 2009;139:87–99.
21. Nimonkar AV, Genschel J, Kinoshita E, Polaczek P, Campbell JL, Wyman C, et al. BLM-DNA2-RPA-MRN and EXO1-BLM-RPA-MRN constitute two DNA end resection machineries for human DNA break repair. Genes Dev 2011;25:350–62.
22. Robison JG, Lu L, Dixon K, Bissler JJ. DNA lesion-specific co-localization of the Mre11/Rad50/Nbs1 (MRN) complex and replication protein A (RPA) to repair foci. J Biol Chem 2005;280:12927–34.
23. Sung P, Robberson DL. DNA strand exchange mediated by a RAD51-ssDNA nucleoprotein filament with polarity opposite to that of RecA. Cell 1995;82:453–61.
24. Schlegel BP, Jodelka FM, Nunez R. BRCA1 promotes induction of ssDNA by ionizing radiation. Cancer Res 2006;66:5181–9.
25. Mosor M, Zióøkowska I, Pernak-Schwarz M, Januszkiewicz-Lewandowska D, Nowak J. Association of the heterozygous germline I171V mutation of the NBS1 gene with childhood acute lymphoblastic leukemia. Leukemia 2006;20:1454–6.
26. Rozonowski K, Januszkiewicz-Lewandowska D, Mosor M, Pernak M, Litwiniuk M, Nowak J. I171V germline mutation in the NBS1 gene significantly increases risk of breast cancer. Breast Cancer Res Treat 2008;110:343–8.
27. Ziolkowska I, Mosor M, Wierzbicka M, Rydzanicz M, Pernak-Schwarz M, Nowak J. Increased risk of larynx cancer in heterozygous carriers of the I171V mutation of the NBS1 gene. Cancer Sci 2007;98:1701–5.
28. Nowak J, Mosor M, Zióøkowska I, Wierzbicka M, Pernak-Schwarz M, Przyborska M, et al. Heterozygous carriers of the I171V mutation of the NBS1 gene have a significantly increased risk of solid malignant tumours. Eur J Cancer 2008;44:627–30.
29. Kanka C, Brozek I, Skalska B, Siemiatkowska A, Limon J. Germline NBS1 mutations in families with aggregation of breast and/or ovarian cancer from north-east Poland. Anticancer Res 2007;27:3015–8.
30. Bogdanova N, Schürmann P, Waltes R, Feshchenko S, Zalutsky IV, Bremer M, et al. NBS1 variant I171V and breast cancer risk. Breast Cancer Res Treat 2008;112:75–9.
31. Taylor GM, O'Brien HP, Greaves MF, Ravetto PF, Eden OB. Mutations in the Nijmegen breakage syndrome gene (NBS1) in childhood acute lymphoblastic leukemia. Cancer Res 2003;63:6563–4.
32. Demuth I, Frappart PO, Hildebrand G, Melchers A, Lobitz S, Stöckl L, et al. An inducible null mutant murine model of Nijmegen breakage syndrome proves the essential function of NBS1 in chromosomal stability and cell viability. Hum Mol Genet 2004;13:2385–97.
33. Chen L, Nievera CJ, Lee AY, Wu X. Cell cycle-dependent complex formation of BRCA1.CtIP.MRN is important for DNA double-strand break repair. J Biol Chem 2008;283:7713–20.
34. Gupta GP, Vanness K, Barlas A, Manova-Todorova KO, Wen YH, Petrini JHJ. The Mre11 complex suppresses oncogene-driven breast tumorigenesis and metastasis. Mol Cell 2013;52:353–65.

Published OnlineFirst May 15, 2014; DOI: 10.1158/0008-5472.CAN-13-3037

AACR American Association for Cancer Research

Cancer Research

The Journal of Cancer Research (1916–1930) | The American Journal of Cancer (1931–1940)

A Rare Polymorphic Variant of *NBS1* Reduces DNA Repair Activity and Elevates Chromosomal Instability

Yuki Yamamoto, Mamiko Miyamoto, Daisuke Tatsuda, et al.

Cancer Res 2014;74:3707-3715. Published OnlineFirst May 15, 2014.

nature genetics

Large-scale genetic study in East Asians identifies six new loci associated with colorectal cancer risk

Ben Zhang[1], Wei-Hua Jia[2], Koichi Matsuda[3], Sun-Seog Kweon[4,5], Keitaro Matsuo[6], Yong-Bing Xiang[7], Aesun Shin[8,9], Sun Ha Jee[10], Dong-Hyun Kim[11], Qiuyin Cai[1], Jirong Long[1], Jiajun Shi[1], Wanqing Wen[1], Gong Yang[1], Yanfeng Zhang[1], Chun Li[12], Bingshan Li[13], Yan Guo[14], Zefang Ren[15], Bu-Tian Ji[16], Zhi-Zhong Pan[2], Atsushi Takahashi[17], Min-Ho Shin[4], Fumihiko Matsuda[18], Yu-Tang Gao[7], Jae Hwan Oh[19], Soriul Kim[10], Yoon-Ok Ahn[9], Genetics and Epidemiology of Colorectal Cancer Consortium (GECCO)[20], Andrew T Chan[21,22], Jenny Chang-Claude[23], Martha L Slattery[24], Colorectal Transdisciplinary (CORECT) Study[20], Stephen B Gruber[25], Fredrick R Schumacher[25], Stephanie L Stenzel[25], Colon Cancer Family Registry (CCFR)[20], Graham Casey[25], Hyeong-Rok Kim[26], Jin-Young Jeong[11], Ji Won Park[19,27], Hong-Lan Li[7], Satoyo Hosono[6], Sang-Hee Cho[28], Michiaki Kubo[17], Xiao-Ou Shu[1], Yi-Xin Zeng[2] & Wei Zheng[1]

Known genetic loci explain only a small proportion of the familial relative risk of colorectal cancer (CRC). We conducted a genome-wide association study of CRC in East Asians with 14,963 cases and 31,945 controls and identified 6 new loci associated with CRC risk ($P = 3.42 \times 10^{-8}$ to 9.22×10^{-21}) at 10q22.3, 10q25.2, 11q12.2, 12p13.31, 17p13.3 and 19q13.2. Two of these loci map to genes (*TCF7L2* and *TGFB1*) with established roles in colorectal tumorigenesis. Four other loci are located in or near genes involved in transcriptional regulation (*ZMIZ1*), genome maintenance (*FEN1*), fatty acid metabolism (*FADS1* and *FADS2*), cancer cell motility and metastasis (*CD9*), and cell growth and differentiation (*NXN*). We also found suggestive evidence for three additional loci associated with CRC risk near genome-wide significance at 8q24.11, 10q21.1 and 10q24.2. Furthermore, we replicated 22 previously reported CRC-associated loci. Our study provides insights into the genetic basis of CRC and suggests the involvement of new biological pathways.

CRC is a leading cause of cancer morbidity and mortality worldwide[1]. It is well established that genetic factors have an important role in the etiology of CRC[2,3]. Deleterious germline mutations in known susceptibility genes, notably *APC* (adenomatous polyposis coli), *MLH1*, *MSH2*, *MSH6* and *PMS2*, confer high risk of CRC in hereditary cancer syndromes[3–6]. Most sporadic CRC cases, however, do not carry these high-penetrance mutations[3,4]. Since 2007, genome-wide association studies (GWAS) and subsequent fine-mapping analyses conducted in individuals of European descent have identified 21 low-penetrance susceptibility loci associated with CRC risk[7–17]. Together, these common loci explain less than 10% of the familial relative risk of CRC in European populations[13,14]. In a GWAS of 7,456 CRC cases and 11,671 controls conducted as part of the Asia Colorectal Cancer Consortium, we identified 3 new loci at 5q31.1 (near *PITX1*), 12p13.32

[1]Division of Epidemiology, Department of Medicine, Vanderbilt-Ingram Cancer Center, Vanderbilt Epidemiology Center, Vanderbilt University School of Medicine, Nashville, Tennessee, USA. [2]State Key Laboratory of Oncology in South China, Cancer Center, Sun Yat-sen University, Guangzhou, China. [3]Laboratory of Molecular Medicine, Human Genome Center, Institute of Medical Science, The University of Tokyo, Tokyo, Japan. [4]Department of Preventive Medicine, Chonnam National University Medical School, Gwangju, South Korea. [5]Jeonnam Regional Cancer Center, Chonnam National University Hwasun Hospital, Hwasun, South Korea. [6]Department of Preventive Medicine, Kyushu University Faculty of Medical Sciences, Fukuoka, Japan. [7]Department of Epidemiology, Shanghai Cancer Institute, Shanghai, China. [8]Molecular Epidemiology Branch, National Cancer Center, Goyang-si, South Korea. [9]Department of Preventive Medicine, Seoul National University College of Medicine, Seoul, South Korea. [10]Department of Epidemiology and Health Promotion, Institute for Health Promotion, Graduate School of Public Health, Yonsei University, Seoul, South Korea. [11]Department of Social and Preventive Medicine, Hallym University College of Medicine, Okcheon-dong, South Korea. [12]Department of Biostatistics, Vanderbilt University School of Medicine, Nashville, Tennessee, USA. [13]Department of Molecular Physiology and Biophysics, Vanderbilt University School of Medicine, Nashville, Tennessee, USA. [14]Department of Cancer Biology, Vanderbilt University School of Medicine, Nashville, Tennessee, USA. [15]School of Public Health, Sun Yat-sen University, Guangzhou, China. [16]Division of Cancer Epidemiology & Genetics, National Cancer Institute, Bethesda, Maryland, USA. [17]Center for Integrative Medical Sciences, RIKEN, Kanagawa, Japan. [18]Center for Genomic Medicine, Graduate School of Medicine, Kyoto University, Kyoto, Japan. [19]Center for Colorectal Cancer, National Cancer Center, Goyang-si, South Korea. [20]A complete list of members and affiliations appears in the Acknowledgments. [21]Division of Gastroenterology, Massachusetts General Hospital and Harvard Medical School, Boston, Massachusetts, USA. [22]Channing Division of Network Medicine, Brigham and Women's Hospital and Harvard Medical School, Boston, Massachusetts, USA. [23]Division of Cancer Epidemiology, German Cancer Research Center, Heidelberg, Germany. [24]Department of Internal Medicine, University of Utah Health Sciences Center, Salt Lake City, Utah, USA. [25]University of Southern California Norris Comprehensive Cancer Center, University of Southern California, Los Angeles, California, USA. [26]Department of Surgery, Chonnam National University Medical School, Gwangju, South Korea. [27]Department of Surgery, Seoul National University Hospital, Seoul, South Korea. [28]Department of Hemato-oncology, Chonnam National University Medical School, Gwangju, South Korea. Correspondence should be addressed to W.Z. (wei.zheng@vanderbilt.edu).

Received 19 November 2013; accepted 21 April 2014; published online 18 May 2014; doi:10.1038/ng.2985

(near *CCND2*) and 20p12.3 (near *HAO1*) associated with CRC risk[18]. In addition, we discovered a new risk variant in the *SMAD7* gene associated with CRC in East Asians[19]. Over the past 2 years, we have doubled the sample size in the Asia Colorectal Cancer Consortium and conducted a 4-stage GWAS, including 14,963 CRC cases and 31,945 controls, to identify additional susceptibility loci for CRC.

RESULTS

Study overview

We performed a fixed-effects meta-analysis to evaluate approximately 2.4 million genotyped or imputed SNPs on 22 autosomes from 5 GWAS (stage 1) conducted in China, Japan and South Korea, including in total 2,098 CRC cases and 6,172 cancer-free controls (**Supplementary Tables 1** and **2**). There was little evidence of population stratification in these studies (**Supplementary Figs. 1** and **2**), with genomic inflation factor $\lambda < 1.04$ in each of the five studies and the meta-analysis ($\lambda_{1,000} = 1.01$). We selected 8,539 SNPs showing evidence of association with CRC risk ($P < 0.05$) according to prespecified criteria (Online Methods). We also included the 31 risk-associated variants identified by previous GWAS[7–20], resulting in a total of 8,570 SNPs. Of these, 7,113 SNPs were successfully designed using Illumina Infinium assays as part of a large genotyping effort for multiple projects. Using this customized array, we genotyped an independent set of 3,632 CRC cases and 6,404 controls recruited in 3 studies (stage 2) conducted in China. After quality control exclusions, 6,899 SNPs remained for analysis in 3,519 cases and 6,275 controls. We evaluated associations between CRC risk and these SNPs in each study separately and then performed a fixed-effects meta-analysis to obtain summary estimates. Again, we observed little evidence of population stratification, either in the three studies individually ($\lambda < 1.05$) or combined ($\lambda = 1.05$, $\lambda_{1,000} = 1.01$) (**Supplementary Fig. 3**). In a meta-analysis of data from stages 1 and 2, we identified 559 SNPs showing evidence of association at $P < 0.005$. We then evaluated these SNPs using data from a large Japanese CRC GWAS (stage 3) with 2,814 CRC cases and 11,358 controls[20]. Thirty SNPs in 25 new loci were associated with CRC risk at $P < 0.0001$ in the meta-analysis of data from stages 1–3 and at $P < 0.01$ in the meta-analysis of stages 2 and 3. Of these SNPs, 29 were successfully genotyped in an independent sample of 6,532 CRC cases and 8,140 controls from 5 additional studies (stage 4) conducted in China, South Korea and Japan.

Newly identified risk-associated loci for CRC

In the meta-analysis of all data for the 29 SNPs from stages 1–4 with 14,963 CRC cases and 31,945 controls, signals from 10 SNPs, representing 6 new loci, showed convincing evidence of an association with CRC risk at the genome-wide significance level ($P < 5 \times 10^{-8}$), including rs704017 at 10q22.3; rs11196172 at 10q25.2; rs174537, rs4246215, rs174550 and rs1535 at 11q12.2; rs10849432 at 12p13.31; rs12603526 at 17p13.3; and rs1800469 and rs2241714 at 19q13.2 (**Table 1**, **Supplementary Fig. 4** and **Supplementary Tables 3** and **4**). Associations of CRC risk with the top SNPs in each of the six loci were consistent across almost all studies, with no evidence of heterogeneity (**Fig. 1**). With the exception of the intergenic SNP rs10849432 at 12p13.31, the remaining nine newly identified risk-associated variants were located in exonic, promoter, 3′ UTR or intronic regions of known genes (**Table 1**). The linkage disequilibrium (LD) blocks ($r^2 > 0.5$) tagged by rs704017 (10q22.3), rs174537 (11q12.2) and rs1800469 (19q13.2) each span multiple genes (**Supplementary Table 5**). The LD blocks tagged by rs11196172 (10q25.2) and rs12603526 (17p13.3) each lie within a single gene. The LD block tagged by rs10849432 (12p13.31) does not contain any known gene. Stratification analyses of the newly identified risk variants by tumor anatomical site (colon or rectum), population (Chinese, Korean or Japanese) and sex (male or female) did not identify any significant heterogeneity (**Supplementary Tables 6–8**). In addition to the six newly identified loci, three additional regions showed association with CRC risk near genome-wide significance at 8q24.11 (rs6469656; $P = 5.38 \times 10^{-8}$), 10q21.1 (rs4948317; $P = 7.14 \times 10^{-8}$) and 10q24.2 (rs12412391; $P = 7.41 \times 10^{-7}$). Results for all 29 SNPs across stages 1–4 are presented in **Supplementary Table 3**.

We performed conditional analyses for SNPs located within a 1-Mb region centered on the index SNP in each of the six newly identified loci.

Table 1 Summary results for risk variants in the six newly identified loci associated with CRC in East Asians

							Stage 1	Stage 2	Stage 3	Stage 4	Stages 1–4	
Locus	SNP	Gene[a]	Annotation	Position[b]	Alleles[c]	RAF[d]	*P*	*P*	*P*	*P*	OR (95% CI)[e]	*P*[e]
10q22.3	rs704017	*ZMIZ1-AS1*	Intron 3	80,489,138	**G**/A	0.32	0.01	0.01	0.004	9.99×10^{-4}	1.10 (1.06–1.13)	2.07×10^{-8}
10q25.2	rs11196172	*TCF7L2*	Intron 4	114,716,833	**A**/G	0.68	0.03	1.82×10^{-5}	0.03	5.18×10^{-7}	1.14 (1.10–1.18)	1.04×10^{-12}
11q12.2	rs174537	*MYRF*	Intron 24	61,309,256	**G**/T	0.59	0.02	1.33×10^{-5}	1.61×10^{-4}	1.60×10^{-13}	1.16 (1.12–1.19)	9.22×10^{-21}
	rs4246215	*FEN1*	3′ UTR	61,320,875	**G**/T	0.59	0.02	2.29×10^{-6}	1.83×10^{-4}	1.25×10^{-11}	1.15 (1.12–1.19)	7.65×10^{-20}
	rs174550	*FADS1*	Intron 7	61,328,054	**T**/C	0.59	0.01	5.71×10^{-6}	1.83×10^{-4}	2.70×10^{-11}	1.15 (1.12–1.19)	1.58×10^{-19}
	rs1535	*FADS2*	Intron 1	61,354,548	**A**/G	0.59	0.02	7.55×10^{-6}	1.24×10^{-4}	1.20×10^{-11}	1.15 (1.12–1.19)	8.21×10^{-20}
12p13.31	rs10849432	*CD9*	Intergenic	6,255,988	**T**/C	0.82	0.002	0.007	0.06	6.95×10^{-6}	1.14 (1.09–1.18)	5.81×10^{-10}
17p13.3	rs12603526	*NXN*	Intron 1	747,343	**C**/T	0.30	0.02	6.86×10^{-4}	0.08	3.80×10^{-4}	1.10 (1.06–1.14)	3.42×10^{-8}
19q13.2	rs1800469	*TGFB1*	Promoter	46,552,136	**G**/A	0.48	0.002	0.002	6.74×10^{-4}	0.03	1.09 (1.06–1.12)	1.17×10^{-8}
	rs2241714	*B9D2*	Exon 1	46,561,232	**C**/T	0.48	0.003	0.002	0.001	0.02	1.09 (1.06–1.12)	1.36×10^{-8}

RAF, risk allele frequency; OR, odds ratio; CI, confidence interval.

[a]Closest gene(s). [b]Chromosome position (bp) is based on the reference genome in the NCBI database, Build 36. [c]Risk/reference alleles are based on forward allele coding in NCBI, Build 36. OR was estimated on the basis of the risk allele (bold). [d]RAF in controls from all stages combined. [e]The summary OR (95% CI) and *P* value were obtained from a fixed-effects meta-analysis.

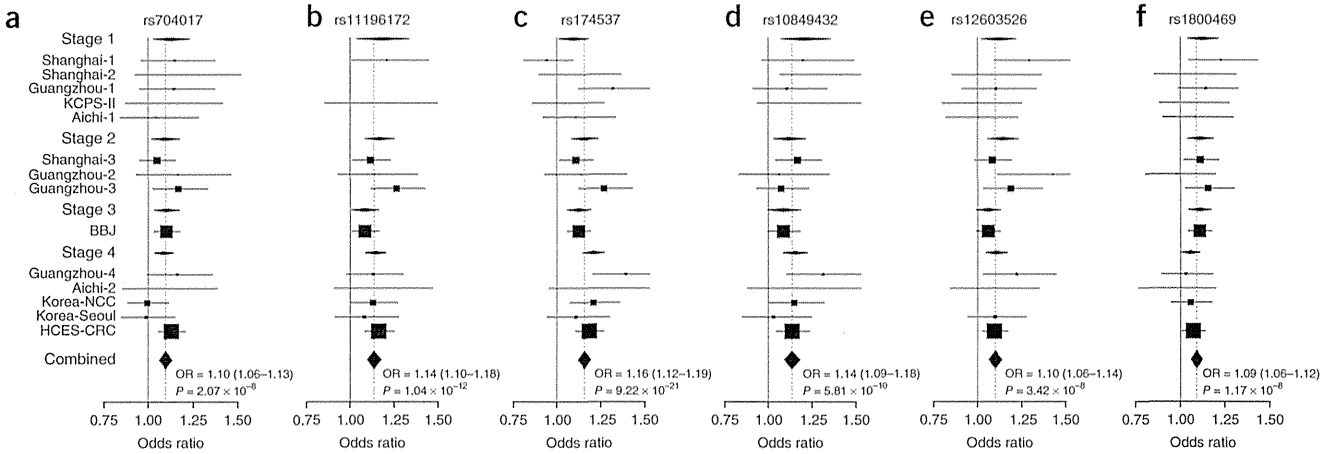

Figure 1 Forest plots for risk-associated variants in the six newly identified loci. (a) rs704017. (b) rs11196172. (c) rs174537. (d) rs10849432. (e) rs12603526. (f) rs1800469. Per-allele OR estimates are presented, with the area of each box proportional to the inverse-variance weight of the estimate. Horizontal lines represent 95% CIs. Diamonds represent summary OR estimates generated under a fixed-effects meta-analysis; width of the diamonds corresponds to 95% CIs. Continuous vertical lines represent the null value; dashed vertical lines represent the summary OR estimates for all studies for each SNP.

No second association signal was identified at $P < 0.01$ after adjusting for the respective index SNP (data not shown). Four SNPs at 11q12.2 and 2 SNPs at 19q13.2 showed association with CRC risk at $P < 5 \times 10^{-8}$, and we thus performed haplotype analysis for these 2 loci using genotype data available for 10,051 CRC cases and 14,415 controls (stages 2 and 4). Two common haplotypes were found in the 11q12.2 locus, accounting for more than 99% of the haplotypes constructed using the four highly correlated SNPs. The haplotype with all four risk-associated alleles (frequency = 0.574 in controls) was strongly associated with CRC risk (odds ratio (OR) = 1.40, 95% confidence interval (CI) = 1.29–1.51; $P = 3.69 \times 10^{-16}$) (**Supplementary Table 9**). Similarly, we identified two common haplotypes at the 19q13.2 locus, accounting for more than 99% of the haplotypes constructed using the two highly correlated SNPs. The haplotype with the risk-associated allele at both SNPs (frequency = 0.485 in controls) was also associated with increased risk of CRC (OR = 1.16, 95% CI = 1.08–1.26; $P = 1.18 \times 10^{-4}$) (**Supplementary Table 10**). Overall, these analyses did not identify an independent signal in any of the six newly identified loci.

We examined potential SNP-SNP interactions between the 6 new risk-associated variants identified in this study (rs704017, rs11196172, rs174537, rs10849432, rs12603526 and rs1800469) and also between these 6 SNPs and the risk-associated variants in 25 previously reported loci (**Supplementary Table 11**). Multiplicative interactions were found with suggestive evidence of association ($P < 0.05$) for seven pairs of SNPs. None of these interactions, however, remained statistically significant after correcting for multiple comparisons in 180 tests (adjusted $P = 0.00028$).

We evaluated associations of the 10 newly identified SNPs with CRC risk in individuals of European descent using data from 3 consortia, the Genetics and Epidemiology of Colorectal Cancer Consortium (GECCO)[17], the Colorectal Transdisciplinary (CORECT) Study and the Colon Cancer Family Registry (CCFR)[21], with a total sample size of 16,984 CRC cases and 18,262 controls (**Supplementary Table 12**). In a meta-analysis of data from these consortia, all ten SNPs showed association with CRC risk in the same direction as observed in East Asians (**Table 2**). Five SNPs in two loci (10q22.3 and 11q12.2) were associated with CRC risk at $P < 0.008$ (corrected for multiple comparisons of six loci). These associations in individuals of European descent, however, were weaker than in East Asians. Tests showed statistically significant evidence of heterogeneity for risk variants at 11q12.2 and 19q13.2 ($P < 0.008$). The frequency of the risk-associated allele was also considerably different in East Asians and individuals of European ancestry for SNPs in five loci (**Supplementary Table 13**). For example, the minor allele (C) of rs12603526 is common in East Asians,

Table 2 Associations of risk variants in the six newly identified loci with CRC in individuals of European descent

Locus	SNP (alleles)[a]	Gene[b]	Position[c]	Cases/controls	RAF[d]	OR (95% CI)[e]	P^e	P_{het}[f]
10q22.3	rs704017 (**G**/A)	*ZMIZ1-AS1*	80,489,138	16,984/18,262	0.57	1.06 (1.03–1.10)	4.71×10^{-4}	0.20
10q25.2	rs11196172 (**A**/G)	*TCF7L2*	114,716,833	7,563/6,328	0.15	1.06 (0.99–1.13)	0.11	0.07
11q12.2	rs174537 (**G**/T)	*MYRF*	61,309,256	16,984/18,262	0.67	1.07 (1.04–1.11)	7.39×10^{-5}	0.001
	rs4246215 (**G**/T)	*FEN1*	61,320,875	16,984/18,262	0.65	1.07 (1.03–1.10)	2.71×10^{-4}	8.31×10^{-4}
	rs174550 (**T**/C)	*FADS1*	61,328,054	16,984/18,262	0.67	1.07 (1.03–1.10)	2.37×10^{-4}	8.87×10^{-4}
	rs1535 (**A**/G)	*FADS2*	61,354,548	16,984/18,262	0.67	1.07 (1.04–1.11)	4.12×10^{-5}	0.002
12p13.31	rs10849432 (**T**/C)	*CD9*	6,255,988	7,563/6,328	0.90	1.03 (0.95–1.11)	0.50	0.03
17p13.3	rs12603526 (**C**/T)	*NXN*	747,343	16,984/18,262	0.02	1.12 (0.98–1.27)	0.10	0.83
19q13.2	rs1800469 (**G**/A)	*TGFB1*	46,552,136	16,984/18,262	0.67	1.03 (1.00–1.07)	0.09	0.01
	rs2241714 (**C**/T)	*B9D2*	46,561,232	16,984/18,262	0.67	1.02 (0.99–1.06)	0.18	0.007

RAF, risk allele frequency; OR, odds ratio; CI, confidence interval.
[a]Risk/reference alleles for East Asians as shown in **Table 1**. OR was estimated for the risk allele (bold). [b]Closest gene(s). [c]Chromosome position (bp) is based on NCBI Build 36. [d]RAF in controls. [e]The summary OR (95% CI) and *P* value were obtained from a fixed-effects meta-analysis. [f]The *P* value for heterogeneity between East Asian and European populations was calculated using a Cochran's *Q* test.